2012

Gold (iii) macrocycles are dna intercalators that inhibit topoisomerase i and ii

Alexander Fagenson
University of Central Florida

GOLD (III) MACROCYCLES ARE DNA INTERCALATORS THAT INHIBIT TOPOISOMERASE I AND II

by

ALEXANDER M. FAGENSON

A thesis submitted in partial fulfillment of the requirements
for the Honors in the Major Program in Microbiology and Molecular Biology
College of Medicine
and in The Burnett Honors College
at the University of Central Florida
Orlando, Florida

Spring Term 2012

Thesis Chair: Dr. Mark T. Muller

Abstract

Human Topoisomerase IB (TOP1) and Topoisomerase IIα (TOP2α) are essential nuclear enzymes that control DNA topology during DNA replication, gene transcription and cell division. These enzymes carry out their catalytic function by making transient single-strand (type I) or double-strand (type II) breaks in the DNA. *In vivo*, these complexes are short-lived but can be exploited by anti-cancer drugs to mechanistically kill cancer cells. Two general classes of compounds can kill cancer cells through a topo-targeted mechanism. Interfacial Poisons (IFPs) act at the enzyme-DNA interface to inhibit the religation reaction, resulting in the accumulation of DNA double-stand breaks (DSBs) in the genomic setting. Catalytic Inhibitor Compounds (CICs) act by interfering with other steps of the catalytic cycles such as DNA/protein binding or the cleavage reaction.

In this work we identify new Au^{3+} macrocyclic gold complexes that act as CICs of both TOP1 and TOP2α. The complexes exhibit square planar geometry with an aromatic system that allows for DNA intercalation with binding affinities in the low micromolar range. A cytotoxicity screen across 60 human cancer cell lines performed by the National Cancer Institute (NCI, USA) reveals significant anti-tumor potential. Our lead compound (butyl gold(III) macrocycle, cmpd 3.) is currently undergoing further studies in animal models at the NCI. *In vitro* assays with purified DNA and enzyme reveal the Au^{3+} ion to be the quintessential switch that allows for DNA intercalation and subsequent inhibition of TOP1 and TOP2α.

Acknowledgements

I would first like to acknowledge Dr. Mark Muller, for his continued guidance and friendship over the past two years. It has been a joy to work in your lab, and thank you for helping me advance my professional career in science. I would also like to thank Dr. Ken Teter for his mentorship throughout the past two years during the PURE and HIM programs. You have given me much feedback and help throughout my time as an undergraduate student, and I really appreciate all the extra time you have spent towards advancing undergraduate research at UCF. I would also like to thank Dr. Dimitry Kolpashchikov for his continued help throughout my thesis project.

Next, I would like to acknowledge Dr. Orde Munro and his graduate student, Kate Akermann; for without them, this work wouldn't exist. Dr. Munro has contributed significantly to this thesis both intellectually and in helping generating some of the figures. Working with you on this collaborative project has been an honor, and I'm glad to be part of the team.

Table of Contents

List of Figures

Chapter 1: Introduction and Background

Classes of Prokaryotic and Eukaryotic Topoisomerases

DNA Topoisomerases are ubiquitous nuclear enzymes that control DNA topology and are required for cell viability[1]. These enzymes are divided into two major types based on the interaction they make with DNA. The type I enzyme is a monomeric unit with a single catalytic tyrosine that cleaves one strand of DNA, performs a controlled rotation, followed by a re-ligation on the cleaved strand. Type II enzymes require ATP and are homodimers containing two catalytic tyrosines. This gives type II the capability of cleaving both strands of DNA resulting in a short-lived DNA double-strand break (DSB). The enzyme then religates the DSB after passing a distant strand through the break. Thus, type I enzymes change the linking number in steps of one, while type II enzymes change the linking number in steps of two[2]. Linking number is an integer that reflects the number of times one strand of DNA is passed through another. Thus the only way to change the value of the linking number is to physically break one (or both) strands of DNA and rejoin them after passing another one through the break, which is accomplished by topoisomerases. The relaxation and decatentation reactions of TOP1 and TOP2α are shown in (**Fig. 1A**).

Both Prokaryotes and Eukaryotes contain Type I and II enzymes. Prokaryotes have a further subdivision in the Type II class that contain DNA Gyrase and Topo IV both of which are A_2B_2 heterotetramers[3]. DNA gyrase is found only in prokaryotic systems and contains a dual function with the ability to induce supercoils into DNA as well as relax supercoiled

DNA. Gyrase is the only topoisomerase known to induce supercoils into DNA rather than remove them. This mechanism is ATP-dependent and can therefore change the linking number of DNA forward or backward in steps of two. DNA gyrase is a well-validated anti-bacterial drug target since humans don't have this protein and it is required for prokaryotes to survive[4]. DNA gyrase is reviewed extensively in the literature [5].

Eukaryotes, on the other hand, don't have a type II enzyme to induce supercoils; they have acquired a nucleosomal complex of DNA and histone proteins allowing DNA to become compact and fit within the nucleus of the cell. In eukaryotes, there are two isoforms of type II enzymes denoted TOP2α and TOP2β[2]. Both of these enzymes have decatenase activity as well as the ability to unknot DNA, which is a type II-specific phenomenon. However, TOP2α is a validated drug-target for cancer chemotherapy, while we are still learning more about the specific role of TOP2β[2]. Eukaryotic Type I topisomerases are broken down into type IA and type IB with the second being the validated drug target. The focus will be on type IB (known as TOP1), as it is the validated drug-target for cancer[5]. TOP1 is also the only enzyme in the topoisomerase family known to form 3' phosphotyrosyl linkages with DNA, whereas the rest of the topoisomerases form 5' linkages[1].

Structure, Function and Catalytic Mechanism of Human Topoisomerase IB (TOP1)

Human TOP1 is an essential enzyme that acts on the chromatin making single-strand DNA nicks to relax supercoiled DNA during various genetic events such as DNA replication, recombination and transcription [6]. TOP1 is a 98 kDa monomeric unit that

begins the catalytic cycle by forming non-covalent interactions with the DNA via H-Bonds to direct itself toward the specific enzyme cut-site. This complex molecular recognition unit is responsible for locking the enzyme onto the DNA prior to formation of the covalent intermediate. Once in correct orientation, the active site tyrosine (Y723) performs a nucleophilic attack on the phosphodiester backbone forming a 3' phosphotyrosyl linkage (unique to humans, as prokaryotes form the 5' linkage). The energy of the supercoil in the DNA drives the controlled rotation of the 5'-OH strand around itself, which is the relaxation step that ultimately changes the linking number by one. The 5'-OH then performs an intramolecular hydrolysis reaction, which is energetically driven by the energy stored in the phosphotyrosyl bond. The catalytic cycle ends when the enzyme releases from the DNA, allowing enzyme turnover and for a new cycle to begin elsewhere[1, 7, 8]. The generalized mechanism for TOP1 mediated relaxation of supercoiled DNA to relaxed DNA is depicted in (**Fig 1C**).

Structure, Function and Catalytic Mechanism of Topoisomerase II (TOP2α)

Human TOP2α and TOP2β are 170 and 180 kDa respectively; both having similar structural properties and features. They require Mg^{2+} and ATP for their catalytic cycle to proceed, and they are homodimers containing two key catalytic tyrosine residues (Y805 and Y821 on the α and β isoform respectively). In the dimerized confirmation TOP2 can sit in either an open or closed clamp conformation dependent on ATP binding. The enzyme dimer has a preference in binding to DNA "nodes" or crossover regions between segements of linked DNA where it selects for a specific alternating purine-pyrimidine sequence. The

catalytic cycle begins when TOP2 localizes and bind to the first strand of DNA, known as the gating segment (G-segment). Following ATP binding, TOP2 undergoes a conformational change to the closed-clamp conformation. Upon binding two Mg^{2+} cations, an ionic/hydrogen bond connection is formed between the phosphodiester backbones, allowing the enzyme to cleave both strands four bases apart via nucleophilic attack of the tyrosines on the phosphodiester. At this point a DNA-DSB has formed, however this "cleavage-complex" is short-lived in cells. The cleavage complex is quickly re-ligated after passing the second strand of DNA known as the Transfer segment (T-segment) through the break. Following ligation of the G-segment, ATP hydrolysis triggers enzyme turnover with a conformational change back to the open-clamp conformation, ready to begin another catalytic cycle[9]. The detailed molecular mechanism and catalytic cycle for TOP2α is presented in (**Figure 1B**).

Figure 1 – Reactions and mechanisms catalyzed by type I and type II topoisomerases

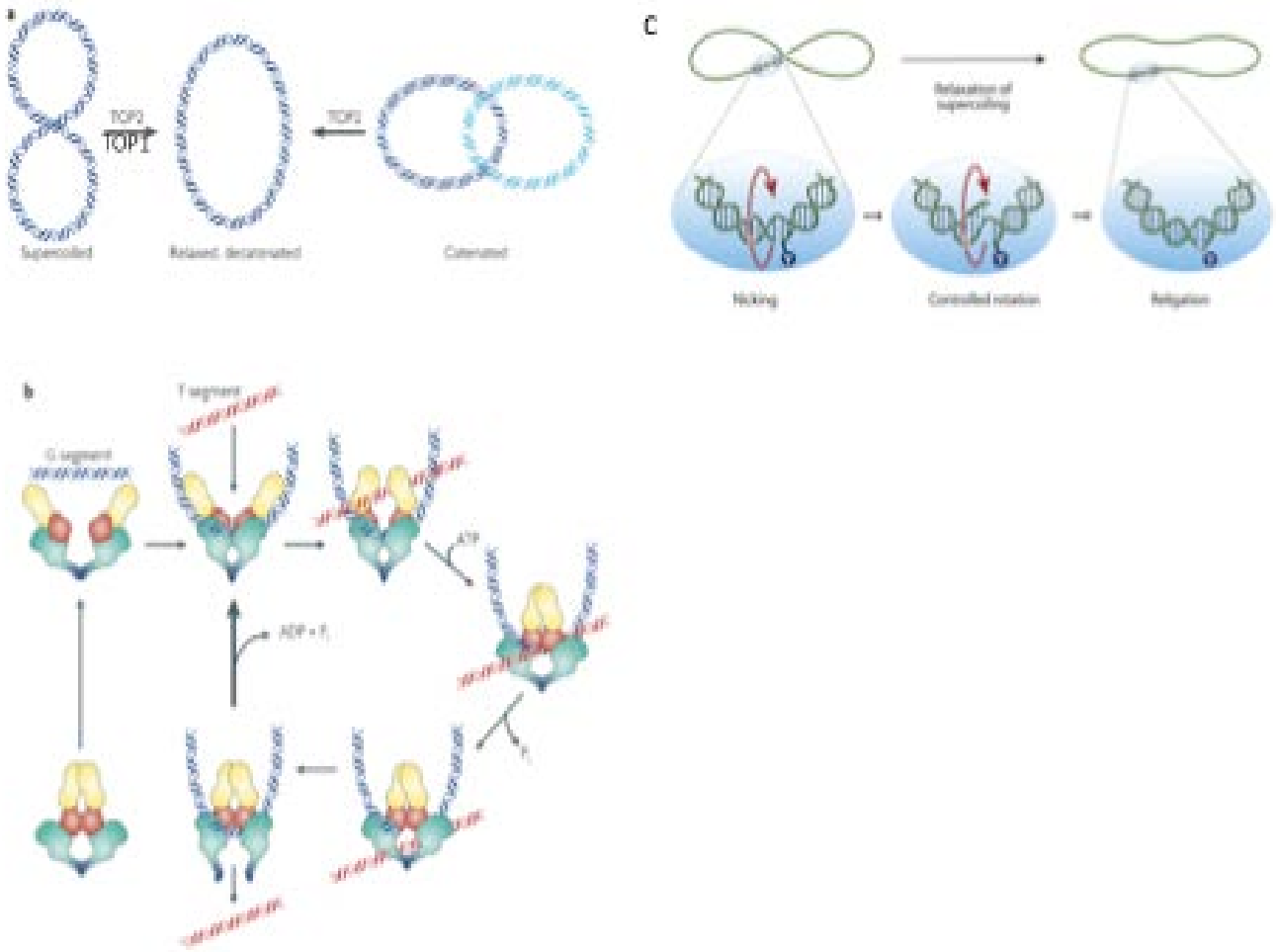

a) TOP1 and TOP2α both have the ability to relax supercoiled DNA. However, TOP2α has decatenase activity, rendering the enzyme capable of unlinking two segments of DNA that are interlocked. Whereby TOP2α takes catenated DNA molecules and turns them to decatenated DNA molecules. This is accomplished by the ability of TOP2α to make a double-strand cut in the DNA and pass a distant segment through the break. [11].

b) Shown here is the stepwise catalytic cycle for TOP2α enzymes. The enzyme cycle involves binding to a DNA segment (G-segment), performing a controlled cleavage of both strands, then passing a distant strand of DNA (T-segment) through the break, followed by religation of the G-segment and hydrolysis of ATP for enzyme turnover [11].

c) The TOP1-mediated relaxation mechanism is shown in panel C. The monomeric enzyme binds to a segment of DNA and cleaves only one strand (through phoosphotyrosine linkage), followed by a controlled strand-rotation step. The enzyme then re-ligates the backbone and leaves the DNA [6].

Involvement of TOP1 and TOP2α in various DNA Metabolic Processes

TOP1 and TOP2α are common drug targets in the clinical setting, especially in cancer chemotherapy[10]. During S phase, DNA replication takes place and with that comes a pressing need for TOP1 and TOP2α . As the replication fork proceeds and DNA helicase separates the two strands, torque is built up in the helix similar to two telephone cords wrapped around each other and pulled apart. This torque generates supercoils ahead and behind the replication fork, and it is the job of TOP1 and TOP2α to relax these supercoils so the replication machinery can operate in a continuous fashion (**Fig 2A**). A similar phenomenon takes place during transcription, as the transcription machinery separates the strands of DNA to read the genetic code. Supercoils are generated ahead of the transcription fork similar to the case in DNA replication. It is the job of TOP1 and TOP2α to relax these supercoils in the same fashion as before [11].

TOP2α plays an important role during mitosis, specifically at the metaphase-anaphase junction. As the chromosomes line up on the metaphase plate and separate as sister chromatids to their respective poles, it is the job of TOP2α to help unlink the chromosomes at the centromere[12]. This vital step in mitosis is highly regulated and shutting down the job of TOP2α will result in failure of proper chromosomal segregation leading to cell death. Also as a result of DNA replication are special structures called catenanes. These catenanes are the result of two separate molecules of DNA inter-locked within one another with a linking number of one. To separate these two pieces of genetic

material we need TOP2α, which can separate the two segments of DNA[2] as shown in (**Fig 2B**).

In conclusion, both TOP1 and TOP2α are at the heart of key events throughout the cell cycle, and for cells to replicate their genome and produce proteins requires TOP1 and TOP2α. Without them, unfavorable DNA superstructures will form that will ultimately result in cell death. This is the premise for why TOP1 and TOP2α are such great targets for cancer therapy.

Figure 2- Importance of topoisomerase in DNA replication and transcription

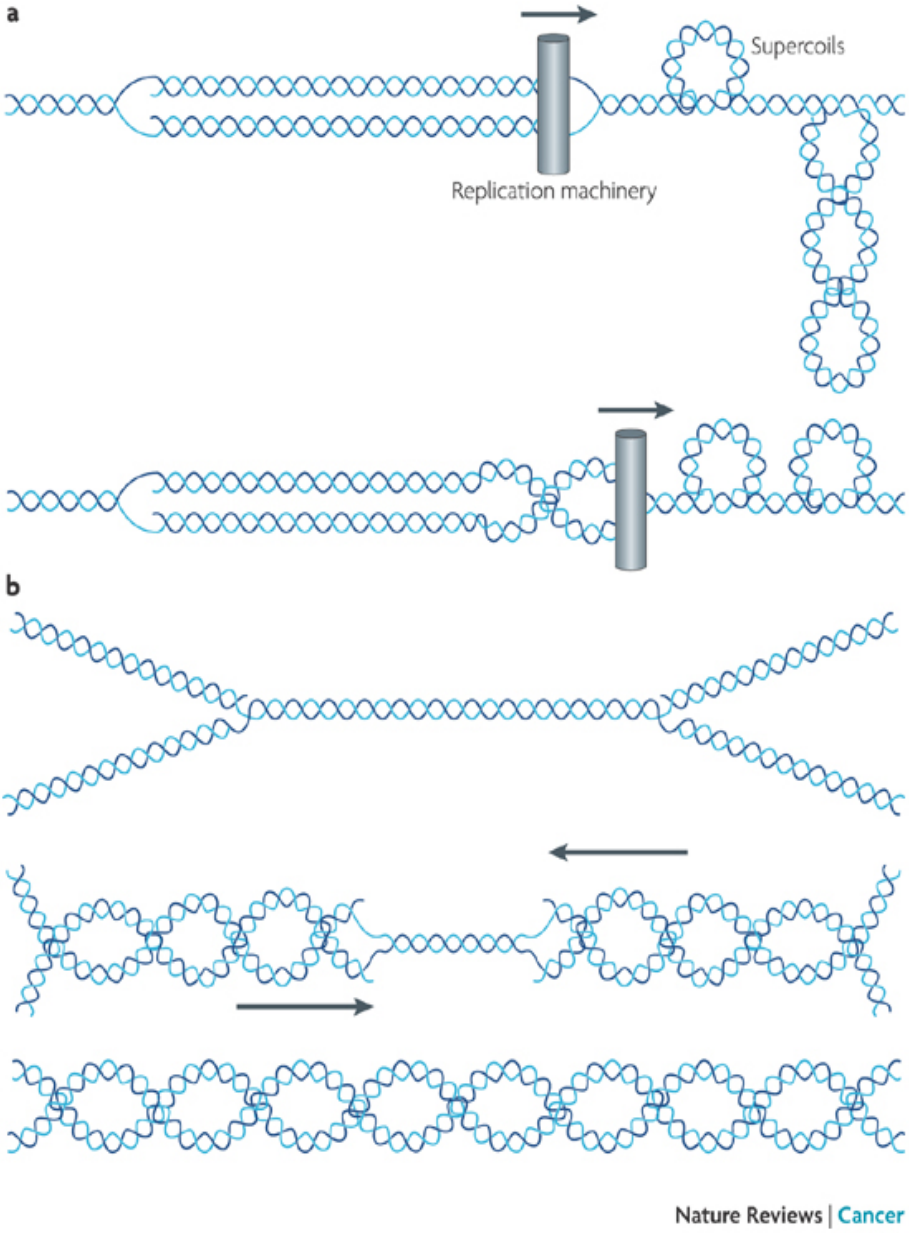

a) As DNA replication and transcription proceeds, supercoils are generated in front of the replication fork as a result of strand separation induced torque. It is the job of TOP1 and TOP2α to relax this DNA, or this will convert to genotoxic lesions upon collision with the replication machinery [11].

b)A result of replication can be the generation of precatenanes which are solely unlinked by TOP2α. These precatenanes, if not decatenated, can be converted to DNA DSBs and ultimately result in cell death [11].

Topoisomerase-Targeted Drugs: Distinction between Catalytic Inhibitors and Interfacial Poisons

Topoisomerase-targeted drugs act through two general mechanisms; as Catalytic Inhibitor Compounds (CICs) and as Interfacial Poisons (IFPs). Most drugs used in the clinic are IFPs, and they act by inhibiting the re-ligation step of the enzyme. These agents stabilize the "cleavage-complex", forming a stable ternary complex between enzyme-DNA-drug. In the genomic context this results in DNA damage that leads to cell death. Poisons can be both type I/II specific. Camptothecin (CPT) is an example of a TOP1 IFP and Etoposide (VP-16) is an example of TOP2α/β IFP. CPT and VP-16 are both widely prescribed in chemotherapy regiments for a plethora of cancers including: breast, colon, leukemia and lymphoma[1, 5, 13]

Drugs that block any other step within the catalytic cycle of TOP1 or TOP2α are referred to as CICs. These compounds are less characterized in the literature, but are of great interest in drug design[12, 14]. CICs have the ability to protect cells from poisoning by the IFPs and can also kill cancer cells without causing direct DNA damage[15, 16]. These CICs can affect the enzyme cycle by either acting with the DNA substrate or the enzyme. A common mechanism involves DNA intercalation by a drug that either blocks the enzyme cut-site or distorts the DNA substrate. This can alter the molecular recognition unit of the enzyme, which makes it unable to lock-on to the DNA to perform a site-specific cleavage event[12, 13]. Another route for CICs can be a small molecule that binds tightly to the enzyme, blocking its ability to either bind DNA or interfere with the cleavage activity. An interesting and well-characterized TOP2α CIC is the family of ICRF compounds

(Bisdioxopiperzine), which cross-link the ATPase domains of TOP2 and keep the enzyme in a closed-clamp conformation[15]. This inhibits the ATP hydrolysis reaction within the catalytic cycle and prevents enzyme turnover, effectively inhibiting future catalytic cycles. Again like IFPs, some CICs are type-specific and some are dual inhibitors. An example of a CIC that operates in a non-intercalative mechanism is Evodiamine[17].

Many anti-cancer agents kill tumor cells through a DNA intercalative mode. This pheneomenon of insertion between the nucleotides of DNA unwinds the helix localized to the intercalation site[18, 19]. Ellipticine and m-AMSA are both DNA intercalators and TOP2α IFPs that utilize their intercalative properties to allow poisoning to occur[20-22]. Intercalation does not always result in a poisoning mechanism as is the case with the anthracyclines (daunorubicin and adriamycin being most common)[23, 24]. These are flat aromatic molecules that intercalate into DNA and add steric bulk to the grooves of DNA. This type of molecular mechanism results in a CIC rather than an IFP due to lack of hydrogen bonding potential[20]. An overview of CICs and and VP-16 a type II IFP are shown below in (**Fig. 3**).

Figure 3 – Drugs that inhibit various steps of the TOP2α catalytic cycle

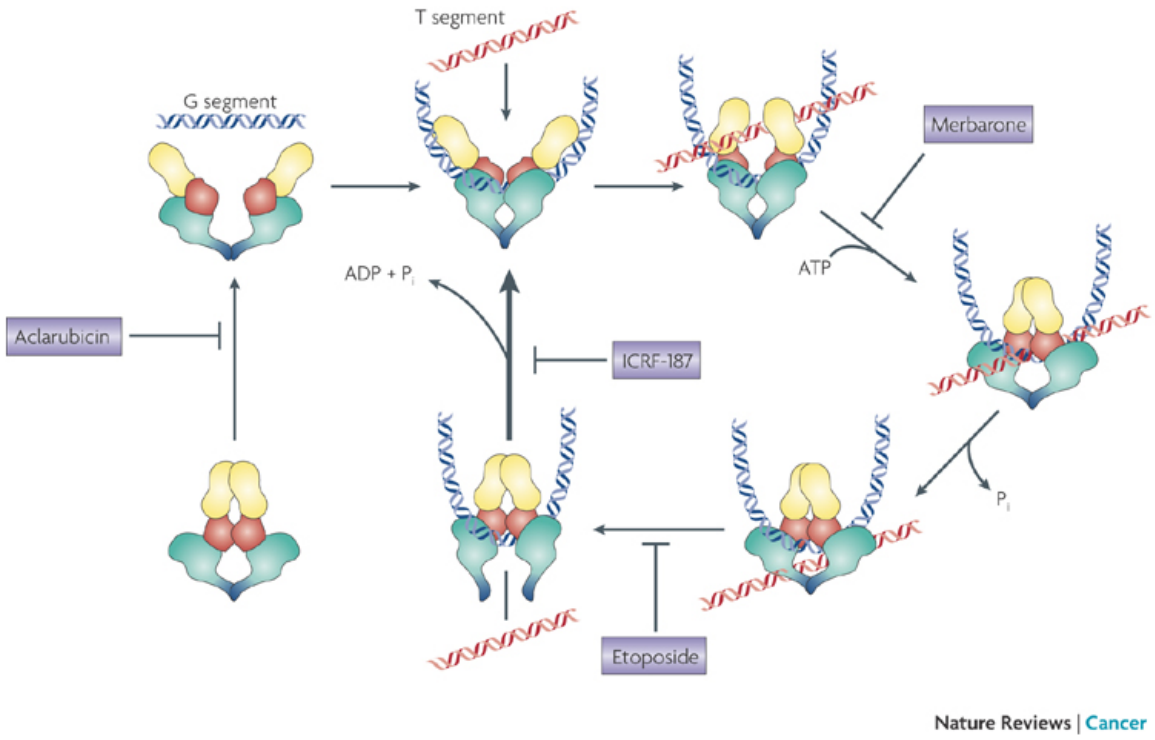

Topo-targeted drugs are classified either as Catalytic Inhibitor Compounds (CICs) or Interfacial Poisons (IFPs). CICs can act on all steps of the catalytic cycle, aside from the religation reaction. Whe IFPs are specific in that they inhibit the religation reaction, joining back the broken segments of DNA. Shown above as an IFP is Etoposide (VP-16), which inhibits the religation reaction of the G-segment. The rest of the drugs shown above are classified as CICs [11].

Metal-Based Drugs in Cancer Chemotherapy

Metal-based drugs have a long history in cancer chemotherapeutics with the most well-studied and characterized being the platinum-based compound, cisplatin. This simple metallo-drug acts in a unique mechanism where it cross-links the strands of DNA by binding to guanine residues seven nucleotides from one another on opposing strands[25]. The Drug-DNA interaction is stable, and can hold the DNA in such a conformation that puts stress on the cell and signals for cell death. This type of interaction along with DNA intercalation is known to induce mutations in the DNA[22]. A pitfall of cisplatin has been the appearance of resistance to this compound, which is believed to be driven by reduced cellular drug-uptake[26]. Moreover, platinum drugs have opened the road to developing other metallo-compounds that bind to DNA. Gold(III) exhibits a square planar geometry with a higher charge, and is believed to help increase the affinity the negatively charged sugar-phosphate backbone of DNA[27, 28]. To date, a number of gold(III) complexes have been synthesized and studied, but few mechanistic details are understood regarding these gold(III) based drugs[29, 30]. Recently gold polypyridyl complexes have been synthesized and are characterized as DNA binders that induce signaling cascades leading to cell cycle arrest and apoptosis[31]. Another group has also synthesized a group of cyclometalted Au^{3+} complexes with N-heterocyclic carbene ligands that were first assigned as TOP1 IFPs, but then shortly after were shown to act as TOP1 CICs[29]. There is thus a pressing need to elucidate the molecular mechanism of these gold-based compounds.

Previous Work and Objective

The objective of the current work is to evaluate a new class of Bis(Pyrrole-Imine) gold(III) macrocycles to see if they target TOP1 and TOP2α. Synthesis of the compounds was carried out by the doctoral student, Kate J. Akermann in the laboratory of Dr. Orde Munro at the University of KwaZulu-Natal (structures shown in **Fig 4**). It has been previously shown in the laboratory through ethidium-bromide displacement assays, that these compounds bind to calf thymus DNA with $K_a > 10^6\ M^{-1}$ (data not shown). The compounds have also been evaluated at the National Cancer Institute (NCI, USA) and show significant cytotoxicty against the NCI Panel of 60 cancer cell lines with GI_{50} (concentration of drug that results in 50% growth inhibition) in the low micromolar range (**Fig 5A)**. Hierarchal cluster analysis performed by Dr. Munro with the leading gold macrocycle (**Fig 5B**, butyl macrocycle, cmpd.3) candidate against 28 FDA-approved cancer drugs with known mechanisms of action in the NCI-60 screen clustered the gold macrocycle next to CPT (TOP1 IFP).

In the following work, we examine the gold(III) macrocycles interaction with DNA *in vitro* using two approaches. Using purified human TOP1 and TOP2α we have measured the cleavage reaction of each enzyme through *in vitro* DNA cleavage assays; to test the inhibitory effects of the gold(III) macrocycles towards the TOP1 and TOP2α enzymes. This mechanistic-based approach will elucidate the *in vitro* molecular mechanism by which gold(III) macrocycles kill cancer cells.

Figure 4- Structures and common names for gold (III) macrocycles synthesized by Kate J. Akermann (Munro Lab)

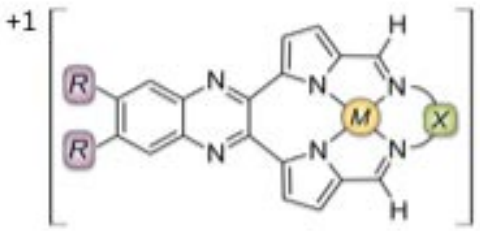

Compound #	M	X	R	"Common-Name"
1, 6, 7	Au, 2H, Ni	$-CH_2CH_2CH_2-$	H	Macro_Propyl_Au, Propyl_, Propyl_Ni
2	Au, Au	$-CH_2C(CH_3)_2CH_2-$	H	Macro_Dimethyl_Au
3	Au	$-CH_2(CH_2)_2CH_2-$	H	Macro_Butyl_Au
4	Au	$-CH_2CHClCH_2-$	H	Macro_Chloro_Au
5	Au	$-CH_2CH_2CH_2-$	CH_3	DM_Macro_Propyl_Au

The gold(III) macrocyclic complexes exhibit square planar geometry with an aromatic system and a net positive charge. The compounds were synthesized and shipped in powdered form. They were dissolved in 100% DMSO and stored as a 20 mM stock at -20°C.

Figure 5-Cytotoxicity data for the butyl gold (III) macrocycle (compound 3) and hierarchal cluster analysis from NCI-60 screen.

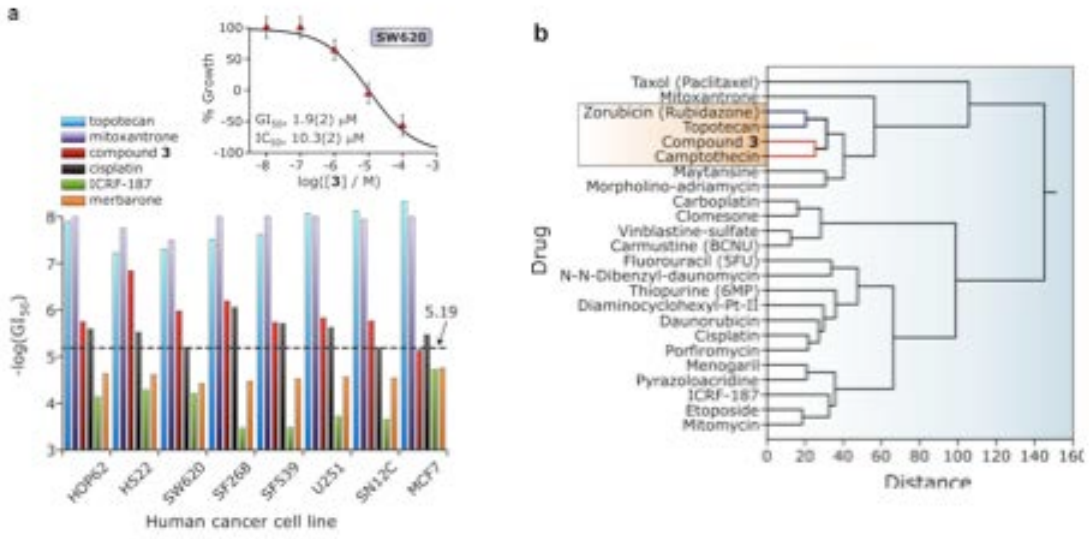

*This figure was produced by Dr. Munro and published under his consent.

a) Cytotoxicity curves of Butyl Complex (compound) against various breast cancer cells in the NCI-60 screen. TOP1 IFP (topotecan),CIC (mitoxantrone) and TOP2 CICs (ICRF-187 and merbarone) are included as a compare reference for chemotherapeutic agents.

b) Hierarchal cluster analysis of various FDA-approved anti-cancer agents, clustered by their GI_{50} values which correlate for mechanism of action as described in chapter 2. The TOP1 IFP, CPT clustered with compound 3 revealing that there might be a possibility of compound 3 targeting TOP1.

Chapter 2: Materials and Methods

Expression and Purification of Human Topoisomerase I

Human TOP1 was expressed as an N-terminal His-tagged protein in a baculovirus system. Experiments were performed with catalytically active wild-type (WT) protein kindly provided by TopoGEN. The protein was purified as described by Stewart and Champoux[32]. Aliquots of protein were stored in a concentration of [0.3 ug/ul] at 4°C in a TOP1 storage buffer (20 mM NaH_2PO_4 pH 7.4, 300 mM NaCl, 50 ug/ml bovine serum albumin, 50% glycerol). One unit of TOP1 will relax approximately 50% of DNA (200 ng of input) in 30 minutes at 37°C. Activity of TOP1 is retained for over six months under proper temperature and storage conditions. A catalytically inactive Topoismerase IB (Y723F) was prepared in which the active site tyrosine was mutated to a phenylalanine. This was kindly provided by TopoGEN and expressed in the same manner.

Expression and Purification of Human Topoisomerase II

Human TOP2α was expressed as a 170 kDa dimer in *Saccharomyces cerevisiae* based on the plasmid YEpTOP2PGAL1 following the protocol from[33]. TOP2α was generously provided by TopoGEN and stored in a TOP2 storage buffer (10% glycerol, 50 mM Tris-HCl pH 7.7, 1 mM PMSF, 2 mM dithiothreitol, 50 ug/ml bovine serum albumin) at -80°C. By definition, one unit of TOP2α will decatenate 200 ng of Kinetoplast DNA (kDNA) in 30 minutes at 37°C. The enzyme can be stored at -80°C and activity can be retained indefinitely so long as freeze-thaw cycles are minimized.

Expression and Purification of DNA Substrates

The catenated DNA substrate, kDNA is a network of interlocked DNA rings harvested from the mitochondria of the insect trypanosome *Crithidia fasciculate*. The kDNA in its catenated form is an aggregation of the interlocked DNA maxicircles and minicircles (~2.5 kb in monomeric form) is unable to pass through the 1% agarose gel. Upon incubation with TOP2α, the minicircles are released as the result of the decatenase activity of the enzyme and its ability to make double-strand cuts in the DNA. The mini-circles migrate through the 1% agarose gel and allow for visualization of the products within the TOP2α catalytic cycle. kDNA is kept in a storage buffer containing (10 mM Tris-HCl pH 7.5 and 1 mM EDTA).

The plasmid pHOT-1 is negatively supercoiled containing a hexadecameric sequence, making it an ideal DNA substrate for TOP1 as described by Bonevan et al[34]. The plasmid itself is a genetically modified PUC12 vector that has the TOP1 high affinity cleavage site (5'-TA-3') inserted into the polylinker region. The pHOT-1 plasmid also contains an ampicilin resistance segment.

Synthesis and Characterization of Gold (III) Macrocycles

Kate J. Akermann carried out the synthesis of the gold complexes in the laboratory of Dr. Orde Q. Munro at the University of KwaZulu-Natal. A total of seven compounds have been synthesized. One of the compounds has a Ni^{2+} ion as the metal (compound. 7) and one is metal free (compound. 6) to serve as controls. The other five all have Au^{3+} ions as their core, with modifications all in the alkyl-bridge portion of the molecule. The derivatives in

the bridge are as follow: Propyl (compound 1), Dimethyl (compound 2), Butyl (compound 3), Chloro (compound 4). The last compound of our library is unique that it contains a further modification of compound 1 on the opposite end of the molecule (quinoxoline region) where the chemists have added two methyl groups (compound 5). The nomenclature and structures of all compounds are summarized in **Fig 4.**

DNA Unwinding Assays

As discussed in chapter 1, DNA intercalation is a common characteristic of many anti-cancer drugs. By intercalating between the bases of DNA, there is an unwinding of the helix and a change in the twist (Tw), which is a measurement of the number of times one strand twists around the other. The Tw is compensated by the writhe (Wr), which is described as the deformation of the DNA double helix in a 3-dimensional plane. The Tw and Wr sum to form a Linking Number (Lk) (Lk = Tw + Wr), which is a fixed integer that describes the number of times one stand is physically linked with the other. Therefore the Lk can only be altered by breaking/resealing the DNA (the action of topoismerases), so intercalative drugs change the Tw and Wr, but not LK. Thus in the presense of TOP1, the changes in tw will be reversed by alterantions in Lk values[35, 36]. This assay allows the distinction between drugs that have the ability to intercalate DNA and those that do not.

DNA unwinding reactions were assembled on ice with 200 ng of supercoiled pHOT-1 plasmid and incubated with 10U of TOP1 for 30 minutes at 37^{o}C in a final volume of 29 ul containing TGS buffer (10 mM Tris-HCl, pH 7.9, 5% glycerol, 0.1 mM Spermidine, 1 mM EDTA, 150 mM NaCl, 0.1% bovine serum albumin). After the incubation, supercoiled DNA

(form I) was converted to relaxed DNA (form I^R). As a positive control, adding SDS to a final concentration of 1% and stopping the reaction after 30 minutes was used as a baseline control for fully relaxed DNA. After the 30-minute relaxation step, designated control and test drugs were added to their specific reaction tubes (final concentration of DMSO = 0.1%) and allowed to incubate for another 30 minutes at 37°C. To account for the DMSO in the drug solutions, a solvent control (DMSO at final concentration of 0.1%) was used to rule out DMSO effects. Reactions were stopped with sodium dodecyl sulfate (SDS) (final concentration. of 1%) and treated with proteinase K (PK) (final concentration of 50 μg/ml) for 30 minutes at 37°C. Following digestion, DNA loading dye was added (0.017 % bromophenol blue, 0.017% xylene cyanofol, 6.67% glycerol) and a phenol-choloroform extraction was performed. An equal volume of Phenol:Chloroform:Isoamyl (PCI) alcohol (25:24:1 w/v) was added and samples were vortexed briefly (10 seconds) and spun for 5 min at 13,000 RPM. The upper phase (aqueous layer) was transferred to a new tube and 33 ng of DNA was loaded onto a 1% agarose gel and electrophoresis was carried out for two hours at 25 volts. The gel was then stained in ethidium bromide (EB) [0.5 mg/ml] for five minutes followed by a de-stain in distilled H_20 and imaged using the GeneSnap Bioimaging system.

DNA Cleavage Assay by TOP1

A modified DNA Cleavage Assay has been developed to study specifically the cleavage reaction of TOP1. TOP1 is in an enzyme that operates on a supercoiled DNA substrate in a catalytic fashion. This can be exploited to show that in the presence of a low-

salt ionic environment and high ratios of TOP1 to DNA, elevated cleavages will be detectable on the agarose gel as the nicked-open circular (form II). Setting up this type of environment will increase the processivity of TOP1 and promote elevated binding to DNA. Optimizing this ratio of TOP1 to DNA can allow one to run a reaction in the presence and absence of test drug and observe if there is a knock-down effect in form II. A reduction in band intensity in form II DNA is consistent with catalytic inhibition. This TOP1 cleavage assay allows for screening of potential CICs. In the presence of CPT, a TOP1 IFP, there will be an increased yield in form II DNA, as well as the appearance of a linear DNA strand (form III). This is owning to the fact that another TOP1 molecule can cut the opposite strand in a concurrent manner (as a result of no salt) having that DNA-break stabilized by another CPT molecule. Thus, in this assay we will see TOP1 IFPs producing linear cleavage complexes, when usually TOP1 cleavage complexes are single-stand breaks *in vivo*.

Cleavage reactions were carried out with 100U of TOP1 and 200 ng of supercoiled pHOT-1 in a 1X TG buffer containing (100 mM Tris-HCl, pH 8, 10 mM EDTA, 1 mM spermidine, 1% bovine serum albumin, 5% glycerol) and indicated drug in a final volume of 30 ul. The zero drug concentration represents a DMSO solvent control (final concentration of 0.1%). Reactions are prepared on ice and initiated with incubation for 30 minutes at 37^{o}C. Following the 30-minute incubation, reactions were stopped by the addition of SDS (final concentration 1%) and digested with PK [50 μg/ml] for 30 minutes at 37^{o}C. DNA loading dye was added (0.017 % bromophenol blue and 6.67% glycerol), and 20 ng of DNA was then loaded onto a 1% agarose gel, which was subjected to electrophoresis

for 1 hour at 50 volts. EB at a final concentration of [0.5 mg/ml] was contained in both the gel and running buffer. The gel was briefly de-stained in distilled H_2O and imaged using the GeneSnap Bioimaging system.

TOP2α Decatenation Assays

A decatenation reaction was performed with kDNA and human TOP2α. Unless otherwise indicated, 200 ng of kDNA was incubated with 4U TOP2α in a TOP2 reaction buffer (50 mM Tris-HCl, pH 8, 150 mM NaCl, 10 mM $MgCl_2$, 0.5 mM DTT, 300 ug/ml BSA, 20 mM ATP) with the indicated amount of control drug or test drug. Reactions were incubated for 30 minutes at 37°C and terminated by the addition of adding SDS (final concentration of 1%) and digesting with PK [50 µg/ml] for 30 minutes at 37°C. DNA loading dye was added (0.017 % bromophenol blue, 0.017% xylene cyanofol 6.67% glycerol) and a phenol-choloroform extraction was performed. An equal volume of Phenol:Chloroform:Isoamyl (PCI) alcohol (25:24:1 w/v) was added and samples were vortexed briefly (10 seconds) and spun for 5 min at 13,000 RPM. The upper phase (aqueous layer) was transferred to a new tube and 50 ng of DNA was loaded onto a 1% agarose gel and subjected to electrophoresis for 20 minutes at 200 volts. EB at a final concentration of [0.5 mg/ml] was contained in both the gel and running buffer. The gel was briefly de-stained in distilled H_2O and imaged using the GeneSnap Bioimaging system.

Surface Plasmon Resonance Analysis

The technique of Surface Plasmon Resonance (SPR) provides a method for measuring and quantifying equilibrium dissociation constants (K_D) in real time. The K_D is

calculated by dividing the dissociation constant (K_d) by the association constant (K_a) [$K_D = K_a/K_d$]. The method utilizes the physical properties of light reflection and electromagnetic wave propagation. Briefly, a light source is focused at a fixed angle with the incident light ray traveling through a prism until it comes into contact with the metal-coated sensor chip. At this point the electromagnetic wave will propagate in the direction parallel to the electromagnetic forces from the chip[37]. The light then makes an angle of reflection that is recorded by the detector after traveling back through the prism. The angle of reflection recorded is thus variable and dependent on what is attached to the chip. In an SPR experiment, a molecule of interest (known as the ligand) is conjugated covalently on the topside of the chip, where the incident ray is focused on the bottom side of the chip. Next a buffer containing your second molecule of interest (known as the analyte) is perfused over the topside of the chip. If there is an interaction between the ligand and analyte then the angle of the light reflecting off the chip will change as the mass on top of the chip increases in value. The detector will record this change in angle, known as the SPR response.

DNA-Drug, Protein-Drug, and Ternary DNA-Drug-Protein interactions were performed using a Reichert SR7000 SPR refractometer (Reichert Inc., Depew, NY, USA). Two sensor chips were utilized in the following experiments, a DNA chip and a TOP1 chip. In the first set of experiments, DNA served as the ligand where a biotinylated twenty base-pair duplexed DNA segment (**Fig. 6**) was immobilized to a neutravidin coated sensor slide (Reichert Inc., Depaw, NY, USA) at a flow rate of 41 µl/min a 1X HBS buffer (10 mM HEPES pH 7.4, 150 mM NaCl and 3 mM EDTA, 10% DMSO). A total of 60 ng of DNA was perfused

over the chip in the HBS buffer to saturate the chip. Gold(III) macrocycles (in a 10% DMSO solution) as analytes were perfused over the DNA chip at a set concentration of 50 nM to check for binding. Macrocycles that bound DNA with a significant SPR response were then titrated over a five-concentration range to establish a K_D. After checking Drug-DNA interactions, TOP1 was perfused over the DNA chip as a control to check for binding to the biotintylated DNA. Then, a combination experiment was carried out where a solution containing Drug-TOP1 was perfused over the DNA chip to determine whether the drug blocked the binding of TOP1 to the DNA.

A protein chip was made with the TOP1 mutant (Y723F) serving as the ligand was conjugated to the sensor slide (Reichert Inc., Depew, NY, USA) via an anti-TOP1 mouse monoclonal antibody (TopoGEN) cross-link. The sensor slide was activated with N-hydroxysuccinimide (NHS) and 1-(3-(dimethylamino)propyl)-3-ethylcarbodimide hydrochloride (EDC) in a 1:1 ratio, which serves as a cross-linker for antibody conjugation to sensor slide via amide chemistry. NHS and EDC were prepared as 0.5 M and 0.2 M EDC solutions in deionized H_20 and stored at -80^oC until the time of the experiment. NHS and EDC were mixed in a 1:1 ratio and perfused over the top of the chip. Following activation, an antibody solution containing 950 ng of TOP1 antibody in a sodium-acetate buffered solution (pH 5.4) was applied on top of the sensor chip. Next 320 ng of TOP1 enzyme was mixed in a solution of 0.05% Tween 20 Phosphate Buffered Saline (PBS-T) which bound with high specificity to the antibody. First, gold(III) macrocycles were perfused over the chip to establish Drug-Protein interactions. Second, the same DNA substrate from the DNA

chip was perfused over the protein chip to check as a control. Third, a solution containing Drug-DNA (equilibrated for 5 min. at 37^{o}C) was perfused over the chip to see if binding of the DNA to the protein was inhibited in the presence of the drug.

Reichert Labview software was used for data collection and Biologic Scrubber 2 software (Campbell, Australia) was used for curve fitting and data analysis. Experiments were performed with assistance from a colleague, Dr. Mike Taylor, Ph.D. (from the lab. of Dr. Kenneth Teter, University of Central Florida), who operated the SPR machine and conducted the data analysis.

Figure 6 – Biotinylated DNA substrate used in binding experiments

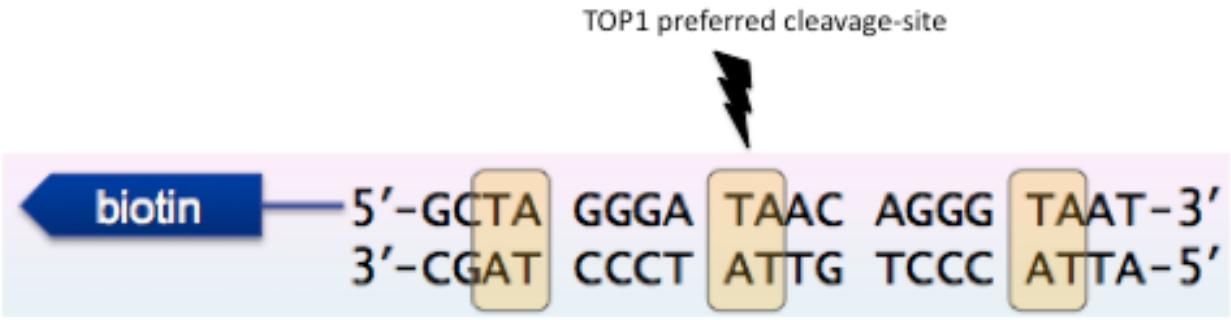

Shown above is the biotinylated DNA substrate used in the SPR experiments. The oligonucleotide contains three 5'-TA-3' dinucleotide sites (boxed in yellow) corresponding to the preferred TOP1 binding site. This is also the hypothesized intercalation site for compound 3. The DNA substrate was immobilized onto the sensor slide through streptavidin-biotin coupling serving as the ligand in the DNA chip. Also, the oligonucleotide was used as the analyte in subsequent experiments, where the DNA was perfused over the TOP1 chip with or without drug.

National Cancer Institute COMPARE Analysis: Cytotoxicity Screen against panel of 60 Cancer Cell Lines

The Developmental Therapeutics Program (DTP) at the National Cancer Institute (NCI,USA) provides a high-throughput screening service of potential anti-cancer agents against a panel of 60-human tumor cell lines. The mission was started in the early 1990s and, as reported by Holbeck et al. has screened over 100,000 compounds and 50,000 natural product extracts [39, 40]. Coupled to the cytotoxicity assay, the NCI has developed a COMPARE algorithm available on their website (dtp.nih.gov) that provides a method to compare your compound of interest against the current FDA-approved anti-cancer agents that are included in the test. The COMPARE algorithim is subject to modification by the investigator, and can be adapted based on the current study.

The details of the cytotoxicity assay can be found on the DTP website at (dtp.nci.nih,gov/branches/btb/ivclsp.html). Briefly, a one-dose screen is initiated by the NCI for preliminary testing. Tumor cells are seeded at a set density in a 96-well plate and incubated at 37^0C in a 5% CO_2 humidifier for one day. After the one day incubation, cells were allowed to reach exponential growth and cell density was recorded via fixation and staining with sulphorhodamine B and processed as the zero time point. To the rest of the plates, designated drugs were added at a final concentration of (1×10^{-5} M), and allowed to incubate for another two days. After the two-day incubation cell density was recorded and processed in the same manner. Growth inhibition of the tumor cells was then calculated

relative to the untreated cells at the zero time-point. This allows for determination of cell killing, and total net growth inhibition.

Dr. Munro performed data interpretation of the NCI-60 cytotoxicity screen and hiercheal cluster analysis via the COMPARE algorithim. The cluster analysis grouped compounds with a known mechanism of action for cell killing using $GI_{50.}$ Shown in (**Fig. 5**) are data from the NCI-60 screen and cluster analysis of the butyl complex (cmpd. 3), performed by Dr. Munro.

Chapter 3: Results

Gold (III) Macrocycles are DNA Intercalators that bind to DNA with a strong affinity

Spectroscopic studies with calf thymus (CT) DNA and gold macrocycles were performed by Kate Akermann prior to receiving the compounds (data not shown). The analysis was performed with a spectrophotometer and measured absorbance changes at 260 nm. CT DNA was intercalated in solution with EB and a peak value was recorded. Various concentrations of the designated gold macrocycle were titrated into solution to measure displacement of the EB by the gold macrocycle. The data reveal that the gold macrocycle specifically displaced EB molecules and bound to CT DNA with an association constant (K_a) in the low micromolar range. Studies with the metal-free macrocycle and nickel-based macrocycle show an inability to displace EB and bind to DNA. This indicated that the Au^{3+} ion allows for a quintessential ionic interaction to take place with the DNA, which allows for DNA binding to occur.

Dr. Munro observed further conformation of DNA binding in a simple gel-shift assay with supercoiled pHOT1 plasmid and the propyl macrocycles. (data not shown). This shift was observed with the propyl gold(III) macrocycle (compound 1), but was not seen with the propyl metal-free macrocycle (compound 6) or the propyl nickel macrocycle (compound. 7). A shift occurs on the gel as a result of the change in molecular weight of complex that is migrating through the 1% agarose gel.

The mode of interaction between the drug and DNA was determined in a DNA unwinding assay (**Fig. 7A**). As described in chapter 2, the DNA unwinding assay measures the various topological states of the DNA in the presence of a DNA intercalator. In the presence of (*m*-AMSA) a known DNA intercalator we see the DNA winding back up in the direction of Form I^R (relaxed DNA) to Form I DNA (supercoiled DNA) (lanes 3-5), which is diagnostic for intercalation. This serves as a positive control and provides a reference for our test compounds. In lanes 6-8 we observe the gold(III) propyl macrocycle (compound 1) intercalating into the DNA and winding it up at lower concentrations as compared to (*m*-AMSA). In lanes 9-14 we observe compounds 6 and 7, metal free and nickel macrocycle respectively; reveal no binding of DNA over the same concentration range. This gives further conformation that the Au^{3+} allows DNA intercalation to occur.

We examined a complete unwinding profile over a wide range titration of the butyl gold(III) complex (compound 3) (**Fig. 7B**). We detected intercalation in the nM range (lanes 8 and 9), as a shift of topoisomers from the form I^R DNA (relaxed) to the form I DNA (supercoiled). In this case, the intercalator winds the DNA back to take on a compact structure. At 5 μM we observe the drug fully winding the DNA (lane 10. The data show that compound 3 intercalation is stronger than (*m*-AMSA) at 5 μM.

Figure 7 – DNA unwinding analysis with gold (III) macrocycles

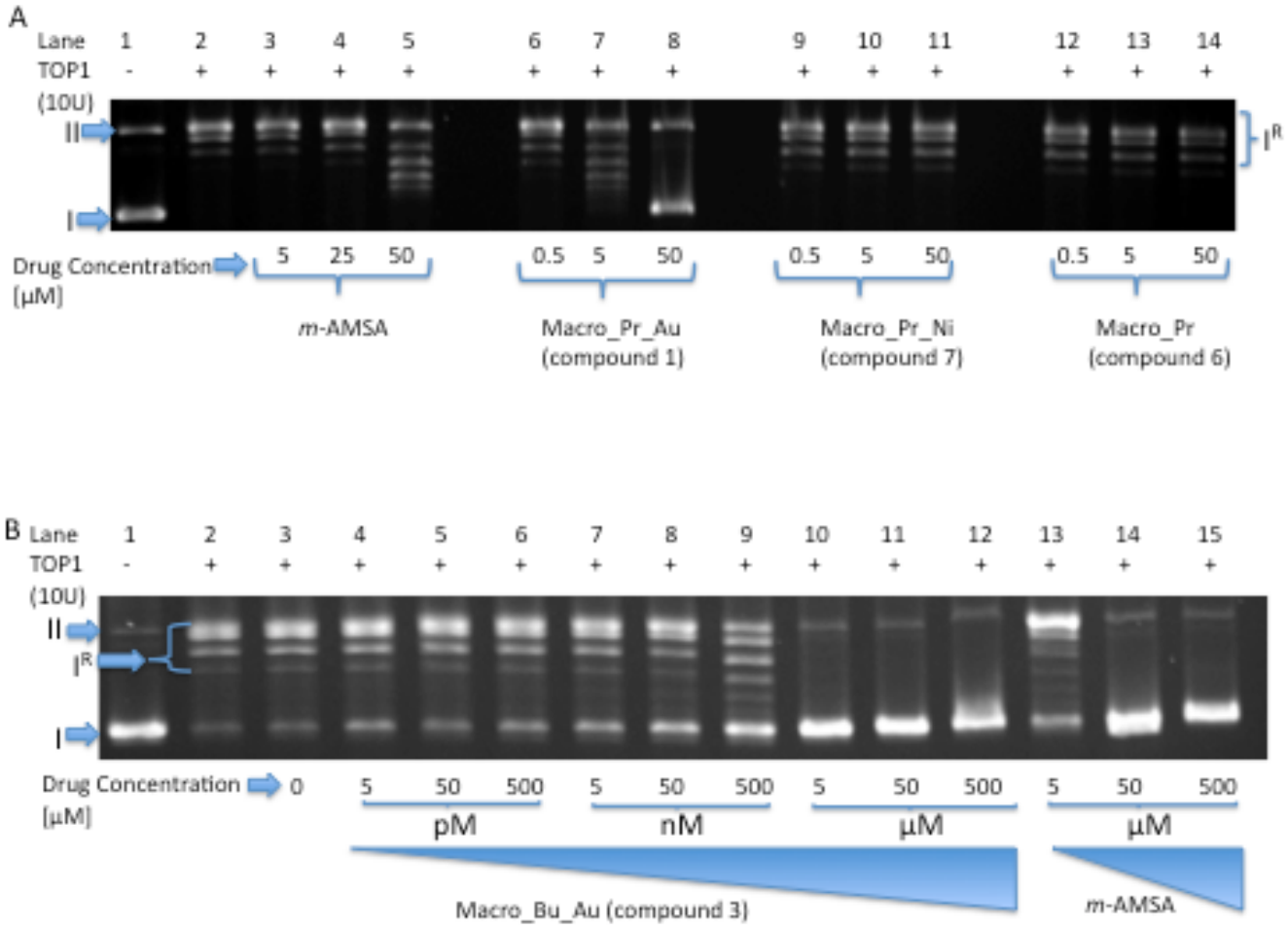

A) A DNA unwinding assay was performed with 200 ng pHOT-1 supercoiled DNA, 10U TOP1 and three propyl macrocycles containing the Au^{3+} cation, Ni^{2+} and the metal-free complex. The forms of DNA are denoted as I(supercoiled), I^R(relaxed), II(nicked-open circular). Lane 1 represents the –TOP1 negative control and lane 2 is the +TOP1 positive control. The reactions were assembled in materials and methods (*m*-AMSA) was used as a positive control for a DNA interclator in lanes 3-5. After fully relaxing the DNA, indicated drug was added and further incubated for 30 minutes. The reactions were stopped with 1% SDS, digested with PK (50 μg/ml) and phenol:chloroform extracted and resolved on a 1% agarose gel for 2 hours at 25V. The gel was then stained in EB [0.5 mg/ml] for 5 minutes and destained in distilled water for 5 minutes. Lane 1 represents the –TOP1 control and lane 2 represents the +TOP1 control. Lanes 3-5 is (*m*-AMSA) over a three-concentration titration. Lanes 4-12 represents a wide range titration of compound 3. Lanes 6-8 represent compound 1, lanes 9-11 show compound 7 and lanes 12-14 show compound 6. All the macrocycles were titrated over the same concentration range [0.5-50 μM].

B) A DNA unwinding assay was performed with 200 ng of pHOT-1 supercoiled DNA,10U of TOP1 and the lead compound, Macro_Bu_Au (compound 3) over a wide titration range in the same manner as described in panel A. The forms of DNA are denoted as I(supercoiled), I^R(relaxed), II(nicked-open circular). Lane 1 represents the –TOP1 negative control and lane 2 is the +TOP1 positive control. Lane 3 represents the solvent control (DMSO, 0.1%). Lanes 4-12 represent compound 3 titrated from pM to μM. Lanes 13-15 show (*m*-AMSA) over a three concentration titration from [5-500 μM]

To quantify the interaction between the DNA and macrocycles, an SPR analysis was conducted with the DNA chip as described in materials and methods. An SPR experiment was performed to monitor binding between the gold(III) macrocycles and DNA using the DNA chip containing the oligonucleotide (see **Fig. 6**). The macrocycles (serving as the analytes) at 50 nM were perfused over the chip in a 10% DMSO solution. The data reveal (**Fig. 8**) reveal that the butyl (compound 3) and propyl (compound 1) gold(III) macrocycles elicited strong SPR responses. We also see additional binding capacities in both of these response curves where binding levels off, followed by additional binding events. With the nickel macrocycle and the metal-free macrocycle, compounds 7 and 6 respectively did not bind to the DNA on the chip (data not shown).

Figure 8 – Gold (III) macrocycles bind to DNA and elicit an SPR response

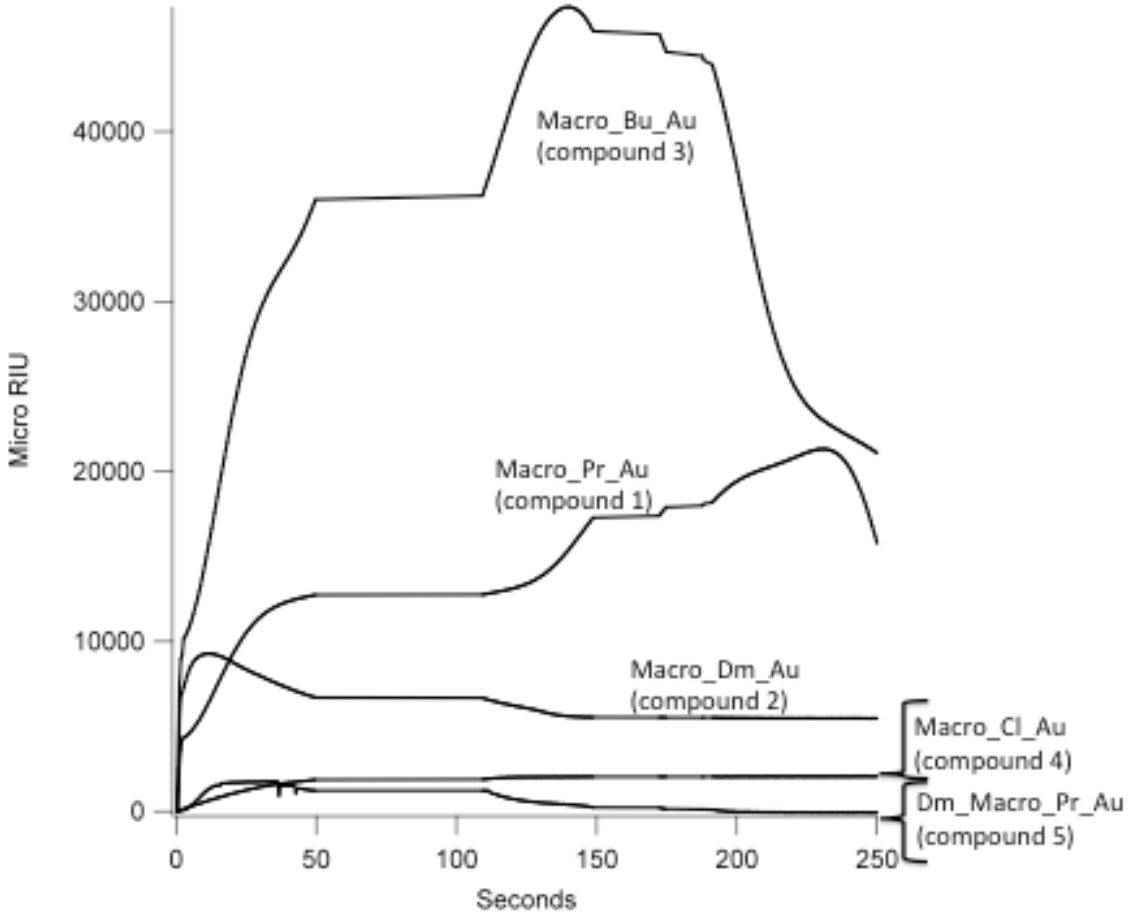

An SPR binding experiment was carried out with the DNA chip as described in chapter 2. In this experiment the various macrocycles were perfused over the chip at 50 nM as the analytes. The oligonucleotide (**Fig. 6**) was covalently conjugated to the sensor chip as the ligand. A total of 100 µl of macrocycles were perfused over the chip and binding was recorded via a response in Micro RIU.

In a second SPR experiment with the DNA chip, the butyl and propyl gold(III) macrocycles, compounds 3 and 1 respectively were titrated over a 4 log-scale to calculate a K_D against DNA. The results of the titration experiment with compounds 3 and 1 are shown below in (**Fig. 9**)**.** The propyl gold(III) macrocycle (compound 1) has a K_D of 2.88 μM and the butyl gold(III) macrocycle (compound 3) has a K_D of 15.32 μM. The data thus show that compound 1 binds to DNA more strongly than compound 3, but within the same order of magnitude. Moreover, the results of **Fig. 8** portray compound 3 to associate with DNA at a much faster rate compared to compound 1. By determining K_D values, we have taken into account both the on-rate (K_a) and off-rate (K_d), measuring a dissociation rate that occurs at equilibrium.

Figure 9 – Propyl and butyl gold (III) macrocycles bind to DNA in a dose-dependent manner

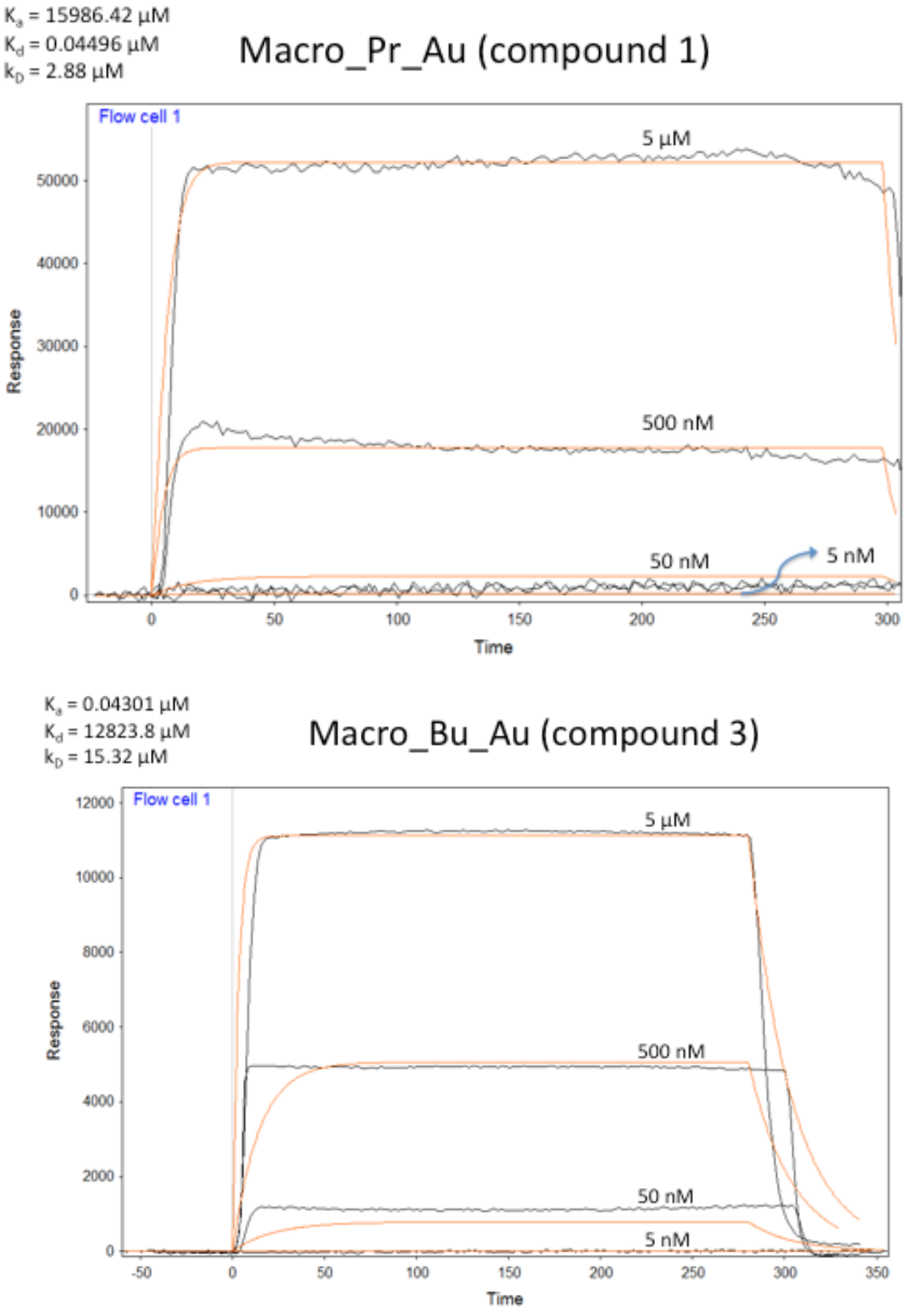

A quantitative SPR experiment was carried out in **Fig. 9** utilizing the propyl and butyl gold(III) macrocycles (compounds 1 and 3 respectively) as analytes and DNA as the ligand. The experiment is carried out with the DNA described in (**Fig. 6**) and as described in materials and methods. A total aliquot of 100 µl of drug was perfused over the DNA chip at a rate of 41 µl/min at 37 ^{0}C.

To test if the gold (III) macrocycles could bind to TOP1, an SPR experiment was performed with the protein chip. Catalytically inactive TOP1 (Y723F mutant) was conjugated to the sensor slide as described in materials and methods to serve as the ligand. The macrocycles were then flown over the protein as the analytes at 50 nM. The butyl gold(III) macrocycle (compound 3) does not bind to the TOP1 protein (**Fig. 10**). The remaining compounds yielded the same results (data not shown). This result demonstrates that the DNA is the primary binding partner for the gold(III) macrocycles, and not TOP1.

Figure 10 – Butyl gold (III) macrocycle does not bind to TOP1

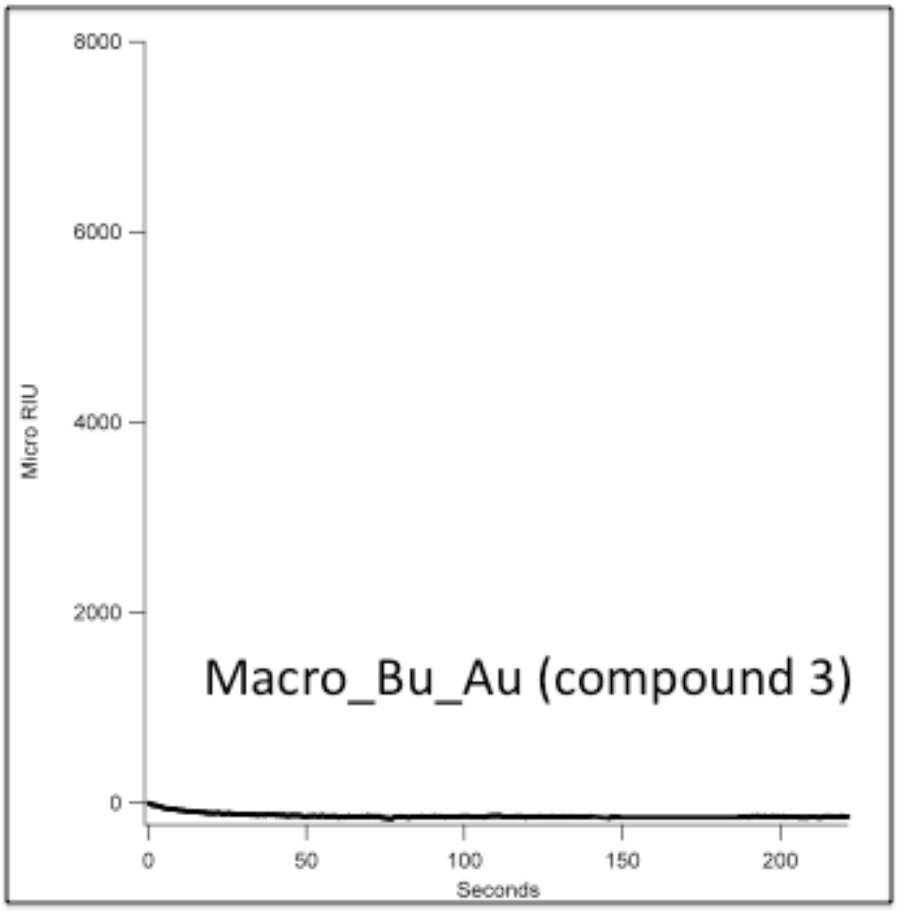

Catalytically inactive TOP1 mutant (Y723F) was attached to the sensor chip, serving as the ligand in the experiment. The butyl gold(III) macrocycle (compound) was perfused over the chip as the analyte at 500 nM in a DMSO solvent . The drug was perfused over the chip at a constant rate of 41µl/min at 37 ^{0}C.

NCI-60 Cytotoxicity Assays and COMPARE Analysis Reveal Significant Anti-Tumor Potential with the Butyl Complex Clustering to TOP1-Targeted Agents

Each of the macrocycles were screened against their panel of 60 human tumor cell lines in a high throughput cytotoxicity assay. Compounds were first put through a one-dose (10 μM) concentration screen to check for gross cytotoxicity in a high throughput screen. Only the butyl gold(III) macrocycle (compound 3) was further titrated over a five-log scale to analyze cell killing over a wider concentration range. Currently, compound 3 has just advanced to animal tumor models in the NCI hollow fiber assays (http://dtp.nci.nih.gov/branches/btb/hfa.html).

The results of the NCI-60 cytotoxicity screen and COMPARE hiercheal cluster analysis of the butyl gold(III) macrocycle (compound 3) is shown in (**Fig. 5**). The results portray significant anti-tumor potential with a GI_{50} values in the low micromolar range. The cluster analysis of the butyl macrocycle (compound 3) next to TOP1-targeted agents (**Fig. 5B**) suggested that TOP1 might be the possible target for the macrocycles. Thus to discern the true mechanism of action, a series of mechanistic-based topoisomerase assays were performed.

Gold (III) Macrocycles are dual Catalytic Inhibitors of TOP1 and TOP2α

A TOP1 DNA cleavage assay was then carried out as described in materials and methods. All seven compounds were analyzed and the results from the lead compound, butyl complex (compound 3) are shown in **Fig. 11.** Five gold compounds (compounds 1-5) effectively inhibited the cleavage activity of TOP1 based on dose-dependent reduction of

nicked-open circular DNA (form II) in **Fig. 11**. The butyl complex (compound 3), which was the most cytotoxic in the NCI-60 screens, yielded an enzyme IC_{50} (concentration that inhibits 50% of the reaction) of 9.2 μM. In lanes 3-8 we titrate the drug over a small scale concentration range and observe a dose-dependent decrease in the yield of Form II DNA The rest of the complexes showed similar inhibitory effects over a similar concentration range with TOP1 being completely inhibited by 20 μM with all gold macrocycles.

In the presence of CPT (a specific TOP1 poison) an increase in the yield of TOP1 cleavage products (form II DNA) as well as the appearance of a linear band (form III DNA), which is predicted under these experimental conditions for the following reason. The low salt and elevated TOP1 promote multiple TOP1 cleavages at nearby cleavage sites. This produces two single-strand nicks that resulted in a double stand break, all stabilized by CPT. A control drug active as a TOP2α IFP (*m*-AMSA) had no effect on the yield of form II or form II cleavage products (**Fig. 11A**, lanes 9-11). This result further confirmed the high specificity of (*m*-AMSA) towards TOP2α, and demonstrates the specificity of our TOP1 DNA cleavage assay. Lanes 13-14 (cropped from another gel) demonstrated the inability of metal-free and nickel complexes (cmpds. 6 and 7) to catalytically inhibit TOP1 at 50 μM.

Figure 11 – Gold (III) macrocycles catalytically inhibit TOP1

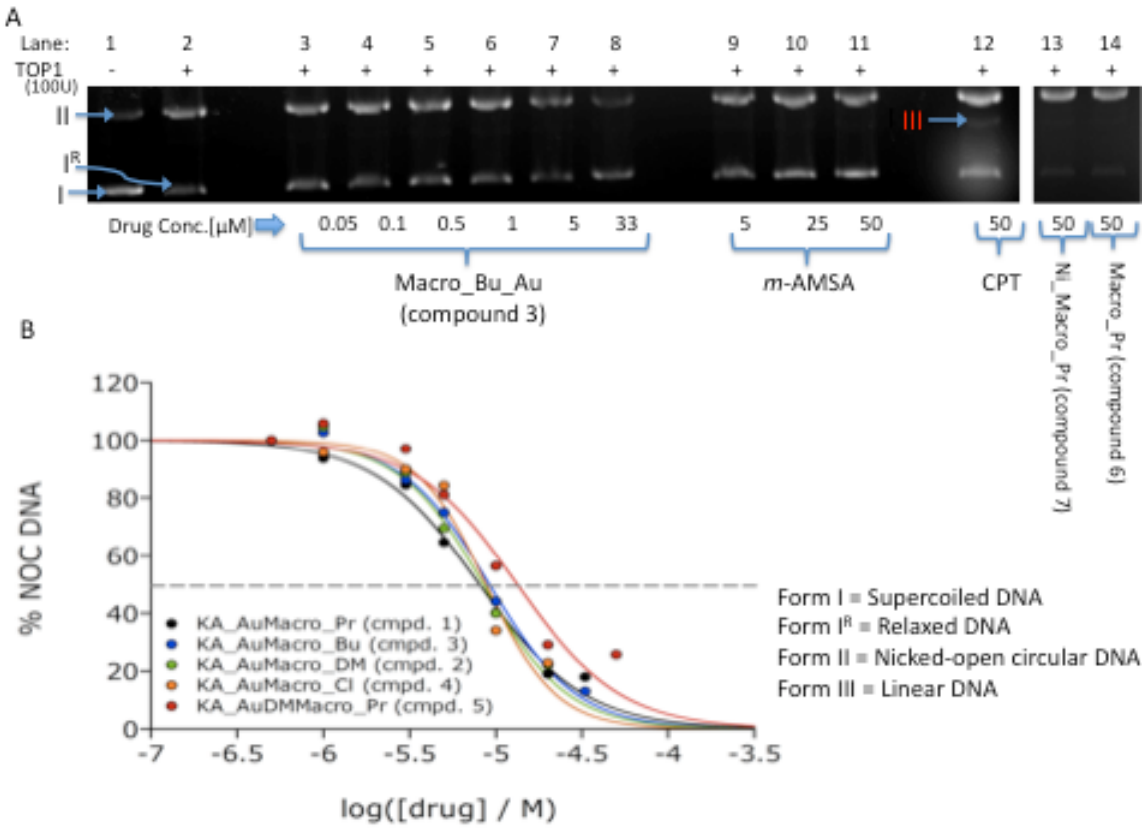

C

Compound	IC_{50} (μM)	R^2 Value	Hill Coe
Macro_Propyl_Au (1)	8.0 (+/- .5)	0.995	1.43 (+
Macro_Dimethyl_Au (2)	8.5 (+/- .6)	0.993	1.76 (+
Macro_Butyl_Au (3)	9.2 (+/- .5)	0.997	1.71 (+
Macro_Chloro_Au (4)	8.8 (+/- .9)	0.981	2.15 (+
DM_Macro_Pr_Au (5)	13 (+/- .2)	0.974	2.45 (+

A) A representative TOP1 DNA cleavage assay as described in chapter 2 is shown of Macro_Bu_Au (compound 3). Briefly, 100U of TOP1 and 200 ng of supercoiled pHOT1 were incubated in a reaction buffer without salt. These conditions allow the enzyme to exhibit enhanced cleavage activity. In lane 1, -TOP1 control, a background level of nicked-open circular DNA (form II) is present as a result from the DNA purification with a predominant amount of supercoiled DNA (form I). In lane 2, the +TOP1 control exhibits an increased yield of form II, which represents the cleavage activity of the enzyme. In lanes 3-8 the butyl complex is titrated across a small concentration range. In lanes 9-11 with (*m*-AMSA) we observe no effect on the TOP1 cleavage reaction. In lane 12, we see CPT (TOP1 IFP) increase the yield of form II DNA as well as the appearance of a linear band (form III), a consistent result due to the experimental conditions. In lanes 13 and 14 cropped from another gel we see that the nickel macrocycle (cmpd. 7) and metal-free macrocycle (cmpd 6.) do not block the catalytic function of TOP1.

B) Graphical representation of inhibition curves for the library of gold(III) macrocycles against TOP1. Quantification of form II DNA (nicked-open circular) in the TOP1 DNA cleavage assays was performed with Genesnap Bioimaging software. Upon substracting the

background signal from lane 1, we set the signal obtained from lane 3 as 100% catalytically active as our reference and divided the band intensities obtained in lanes 4-8 by the value obtained in lane 3 to come up with an IC_{50}(concentration that inhibits the reaction 50%).

C) Summary of data reporting IC_{50}, R^2 and hill coefficient values for the five gold (III) macrocycles from the curve fits in part B. The data analysis was performed with Kyplot and the function used to fit the data is $F(x) = 100/(1+(10^X/A)^B)$ where F(x) is the % of NOC DNA (Form II), x=drug conc., $A=IC_{50,}$ B= hill coefficient. The IC_{50} represents the concentration of drug that results in 50% enzyme activity. The hill coefficient is a positive integer, which represents multiple drug binding sites in the DNA. The data is reported as the result of one independent experiment per drug. The R^2 values of the fits indicate the data are reliable and the +/- comes from the standard deviation of the curve fits based on the R^2 values obtained.

TOP2α decatentation assays were carried out to determine whether the gold(III) macrocycles inhibit or poison this enzyme. Decatenation assays were performed in (**Fig. 12**) as described in materials and methods using VP-16 as the positive control for a TOP2α IFP. The effect of VP-16 poisoning was measured by the appearance of a linear band corresponding to the TOP2-covalent cleavage complex. The propyl (cmpd. 1), dimethyl (cmpd 2.) and butyl (cmpd. 3) gold macrocycles titrated over a wide-range logarithmic scale in a kDNA decatenation is shown in (**Fig. 12A**). The data reveal that gold(III) macrocycles are TOP2α CICs. The enzyme was completely inhibited by 500 μM (**Fig. 12A,**

lane 14) as measured by the retention of the catenated form (cat.) of kDNA in the wells of the 1% agarose gel. The TOP2α decatenation reaction was unaffected by the metal free and nickel macrocycle, compounds 6 and 7 respectively (lanes 6 and 7, **Fig. 12B),** thus confirming the importance of the Au^{3+} ion.

Figure 12 – Gold (III) macrocycles inhibit the TOP2α decatenation reaction

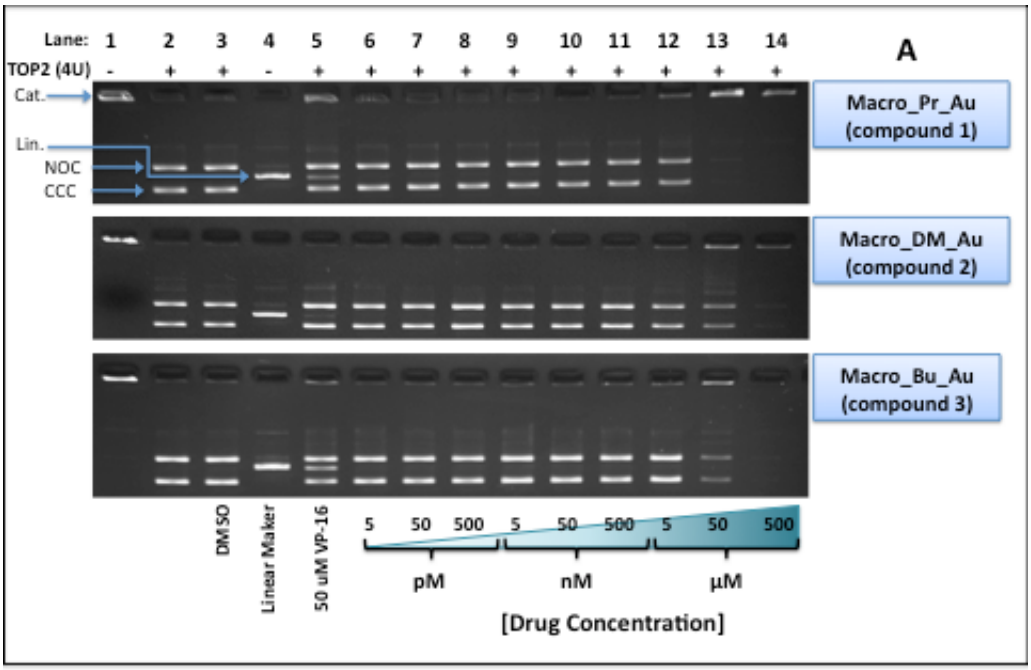

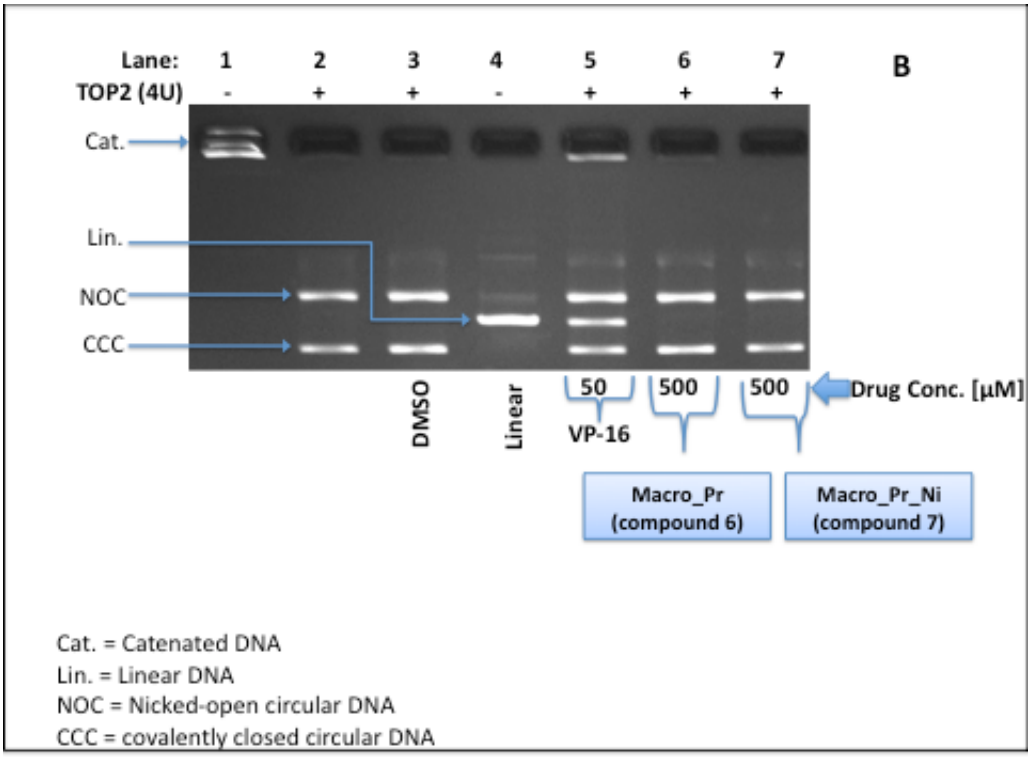

A)

TOP2α reactions were carried out with 200 ng of kDNA and 4U of TOP2α with compounds 1, 2, 3 as described in materials and methods. Reactions were incubated for 30 minutes at 37 ^{0}C, stopped with 1% SDS and digested with PK (50 µg/ml) for another 30 minutes at 37

^{0}C . The reaction products were resolved on a 1% agarose gel containing EB in the gel and running buffer at a concentration of 0.5 mg/ml.The different forms of DNA are denoted as: cat. (catenated DNA), Lin. (linear DNA), NOC (nicked-open circular DNA) and CCC (covalently-closed circular DNA). Lane 1 represents kDNA in its catenated form, unable to travel through the 1% agarose gel. In lane 2, the TOP2α decatenation products are shown producing the NOC and CCC forms of DNA. Lane 3 represents the DMSO (solvent control) at a final concentration of 0.1%. In lane 4, kDNA is linearized by the restriction enzyme Xho1 resulting in a single linear band. Lane 5 is a control for a TOP2α IFP, VP-16 at a final concentration of 50 μM. In lanes 6-14 we observe a wide range titration of the indicated gold(III) macrocycle.

B) TOP2α reactions were carried out with 200 ng of kDNA and 4U of TOP2α with compounds 1, 2, 3 as described in materials and methods. Reactions were incubated for 30 minutes at 37 ^{0}C, stopped with 1% SDS and digested with PK (50 μg/ml) for another 30 minutes at 37 ^{0}C . The reaction products were resolved on a 1% agarose gel containing EB in the gel and running buffer at a concentration of 0.5 mg/ml.The different forms of DNA are denoted as: cat. (catenated DNA), Lin. (linear DNA), NOC (nicked-open circular DNA) and CCC (covalently-closed circular DNA). Lane 1 represents kDNA in its catenated form, unable to travel through the 1% agarose gel. In lane 2, the TOP2α decatenation products are shown producing the NOC and CCC forms of DNA. Lane 3 represents the DMSO (solvent control) at a final concentration of 0.1%. In lane 4, kDNA is linearized by the restriction enzyme Xho1 resulting in a single linear band. Lane 5 is VP-16, serving as a control for a TOP2 IFP at a final concentration of 50 μM. In lanes 6 and 7 we observe the metal free and nickel macrocycle (compounds 6 and 7 respectively) at 500 μM.

DNA Intercalation is the mode of action by which Gold (III) Macrocycles prevent TOP1 from forming a non-covalent complex with DNA

SPR combination experiments were performed by perfusing the TOP1 mutant (Y723F) over the DNA chip in the absence or presence of the butyl gold (III) marcocycle (compound 3). Compound 3 appears to bind DNA in a step wise process (**Fig. 13A)**. In addition, the TOP1 mutant (Y723F) also binds DNA in the absence of the drug (**Fig. 13B)**. When the TOP1-compound 3 solution (50 nM) as the analyte was tested for binding, nonr was observed (**Fig. 13B)**. This reveals that the intercalative gold compound blocks TOP1 from binding to the DNA. A binding event was observed when the TOP1-metal free complex (compound) as the analyte was perfused over the DNA chip, demonstrating that the metal-free macrocycle does not block binding of TOP1 to the DNA (data not shown).

Figure 13- Butyl gold(III) marocycle prevents TOP1 from binding to DNA

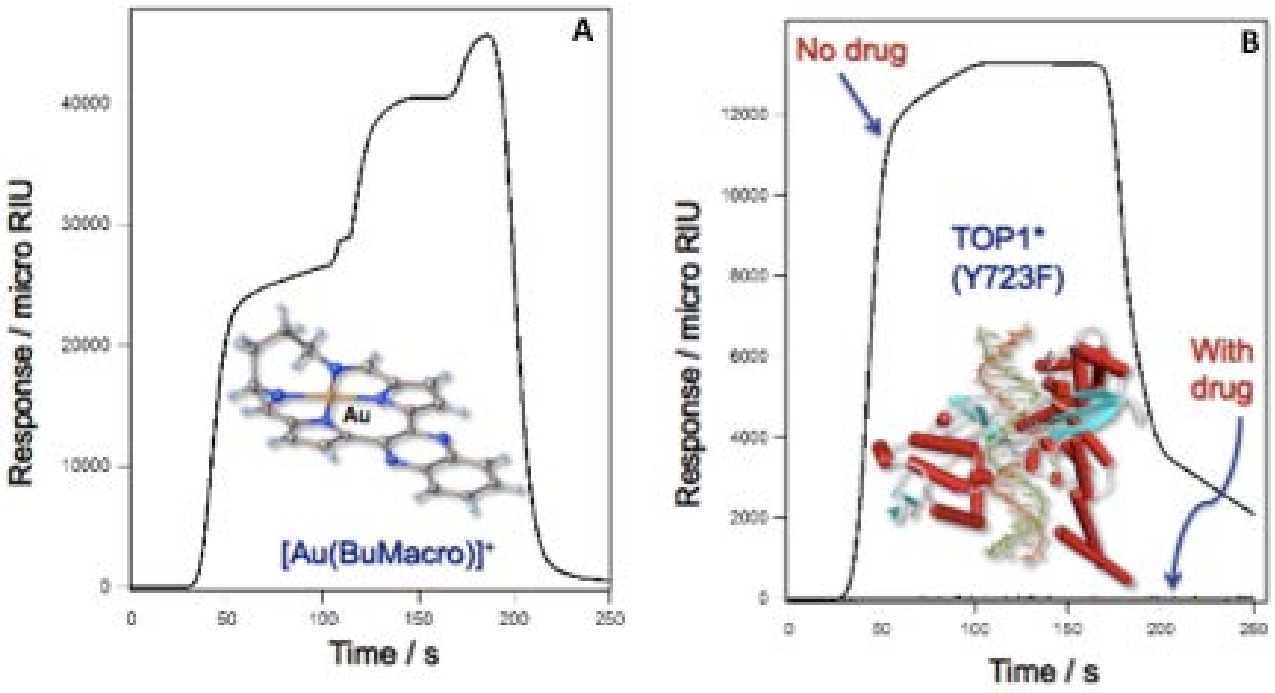

A) An SPR experiment was performed with the DNA chip (sequence shown in **Fig. 6**) in the presence of the butyl gold(III) macrocycle (compound 3). The experiment was conducted by perfusing compound 3 at 50 nM in 10% DMSO over the DNA chip.with cmpd. 3 at 50 nM in a 10% DMSO solution. A total of 100 µl aliquot of drug was perfused over the DNA chip as the analyte.

B) An SPR experiment was performed with the TOP1 mutant (Y723F), to strictly measure the non-covalent complex formed between TOP1 and DNA. An aliquot of 100 µl containing 150 ng of TOP1 was flown over the DNA to check for binding. Then in a second experiment, TOP1 (150 ng) was combined with the butyl gold(III) macrocycle at 50 nM and perfused over the DNA chip as the analyte.

TOP1/DNA interactions were examined in the presence or absence of gold(III) macrocycles by SPR. The SPR response of DNA perfused as the analyte over TOP1 is shown in (**Fig. 14**). In combination experiments, the butyl gold(III) macrocycle (compound 3) was allowed to equilibrate with the DNA for 5 minutes at 37^{o}C. The presence of the gold macrocycle inhibited binding of the DNA to TOP1 (**Fig. 14**). The DNA incubated in the presence of the metal-free macrocycle (compound 6) retained the ability of the DNA to bind to TOP1 (data not shown). By conducting these experiments in reverse manner we confirm our mechanism of action for catalytic inhibition of TOP1. By intercalating into the DNA and not binding the to the enzyme we demonstrate the ability of the gold(III) macrocycle to prevent the formation of a non-covalent complex between DNA and TOP1 via an intercalative phenomenon.

Figure 14 – Butyl gold (III) macrocycle prevents DNA from binding TOP1

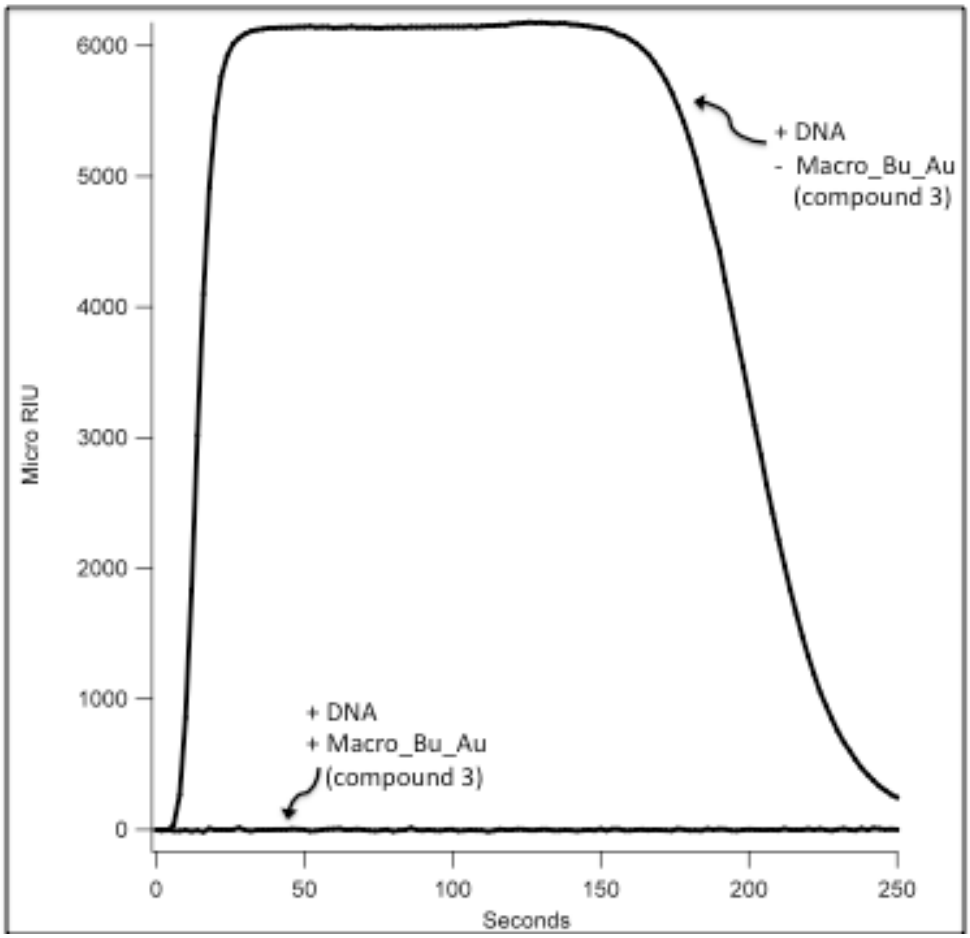

A competition SPR experiment was carried with the TOP1 chip. DNA alone as the sole analyte (oligonucleotide described in **Fig. 6**) was perfused over the TOP1 chip. The DNA was then pre-incubated with the butyl gold(III) macrocycle (compound 3) at 50 nM for 5 min. at 37 ^{0}C and perfused over the chip.

Butyl Gold (III) Macrocycle prevents formation of TOP1-Covalent Cleavage Complex by CPT

A TOP1 DNA Cleavage Assay was performed with the butyl gold (III) macrocycle (compound 3) in the presence of CPT (**Fig. 15**). The results in (**Fig. 11**) demonstrate that compound 3 is a TOP1 CIC that accomplishes its mechanism through an intercalative mode. Since the inhibition of TOP1 takes place at the step of DNA binding to protein, we asked the question if cmpd. 3 could effectively inhibit the CPT-induced TOP1 cleavage complex. In the presence of CPT [100 μM] we measured formation linear band (form III) (**Fig. 15**, lanes 6-8) with increasing enzyme input. Due to low ionic conditions (no salt in the reaction buffer) the enzyme is highly processive, which enchances TOP1/DNA binding and promotes contiguous cutting of the DNA at nearby sites or opposite stands. This leads to formation of linear (form III) DNA. Intercalation of compound 3 effectively blocks this event. By inhibiting formation of the TOP1-CPT induced cleavage complex we confirm that compound 3 and CPT are both localized to the enzyme's cut-site. Although, we cannot rule out the fact that intercalation sites distal to the enzyme-cut site can also result in the prevention of CPT induced cleavage complex.

Figure 15 – CPT induced TOP1 cleavage complex formation is inhibited by butyl gold (III) macrocycle

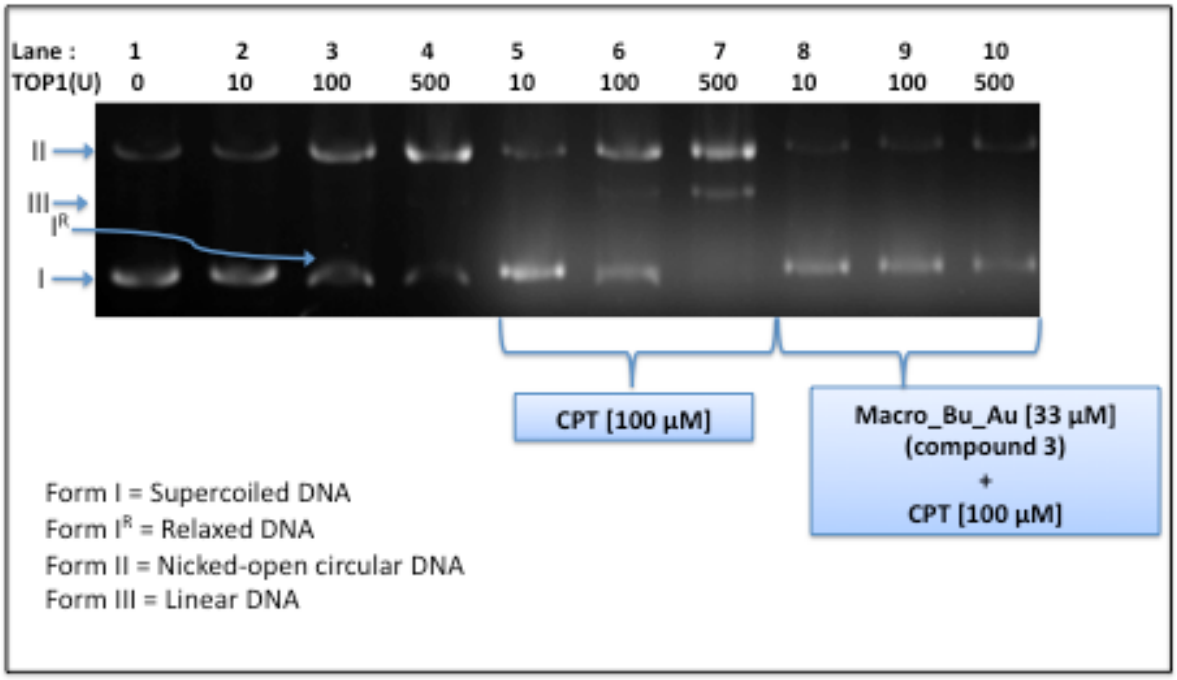

A TOP1 DNA cleavage assay was carried with out with supercoiled 200 ng of pHOT1 DNA and indicated amounts of TOP1 as described in materials and methods: Form I represents supercoiled DNA, form I^R is relaxed DNA, form II is nicked-open circular DNA and form III represents linear DNA. Lane 1 represents mostly form I DNA in the absence of enzyme or drug to show the background level of form II DNA as a result from the DNA purification. The enzyme is then titrated in lanes 2-4 to show the increase in form II. In the presence of CPT [100µM], lanes 5-7 we see a dose dependent increase in form III. In lanes 8-10, the butyl gold (III) macrocycle [33 µM] (compound 3) is incubated in the presence of CPT.

Chapter 4: Discussion

In this work, we have identified the molecular basis by which gold(III) macrocycles act as TOP1 and TOP2α catalytic inhibitors (CICs). DNA intercalation is the primary mechanism by which the gold (III) macrocycles inhibit these enzymes. Most likely, the inhibition is accomplished by distorting the geometry of the enzyme cut-site, impairing the ability of the enzyme to bind to its substrate and perform its catalytic reaction. At the moment, the sequence-specificity of the gold(III) macrocycles is being determined via molecular simulations

Preliminary results from the simulations with the butyl gold(III) macrocycle (compound 3) (**Fig. 16**) suggests that the complex targets a "TA" di-nucleotide via the major groove, corresponding to the cut-site for TOP1[13]. Viewed in **Fig. 16A** is the DNA unbound and and in complex with compound 3. The molecular surface representation reveals cmpd. 3 to intercalate into the DNA as predicted, and fit the contour of the major groove of DNA. This alters the shape of the DNA and adds steric bulk to the DNA, which distorts the substrate for the enzyme. The molecular recognition unit of the enzyme then fails to recognize its sequence-specific cut-site. The sequence was determined via thermodynamic values obtained in the simulation that rendered the "TA" intercalation site in the lowest energy conformation, translating to the most stable complex. A co-crystallization experiment with DNA and compound 3 could confirm this result. Nucleotide specificity may play an important role in regards to cell cytotoxicity.

In addition to base-pair specificity, the simulation work also provides a valid reason why the gold (III) macrocycles bind to DNA (and not the gold-free macrocycle, compound 6). The simulation data reveals a non-traditional interaction seen with the Au^{3+} and the carbonyl oxygen on the thymine residue (**Fig 16B**). The 3.1Å bond formed resembles that of a hydrogen bond, where in this case the Au^{3+} accepts an electron pair donated by the carbonyl oxygen. Originally it was hypothesized that the Au^{3+}cation would interact with negative charges on the sugar-phosphate backbone, however the simulations suggests otherwise. If the gold cation is left out of the macrocycle; the π-π interactions between drug and bases of DNA are not sufficient enough to form a stable complex. Based on the simulation data we would conclude the two main driving forces for compound 3 binding to DNA is, an Au^{3+}--(O=C) 3.1 Å bond in conjunction with stable π-π interactions of the macrocycle to the base-pairs above and below the intercalation site.

Figure 16 – Molecular simulation of butyl gold(III) macrocycle intercalated into DNA (produced by Dr. Munro)

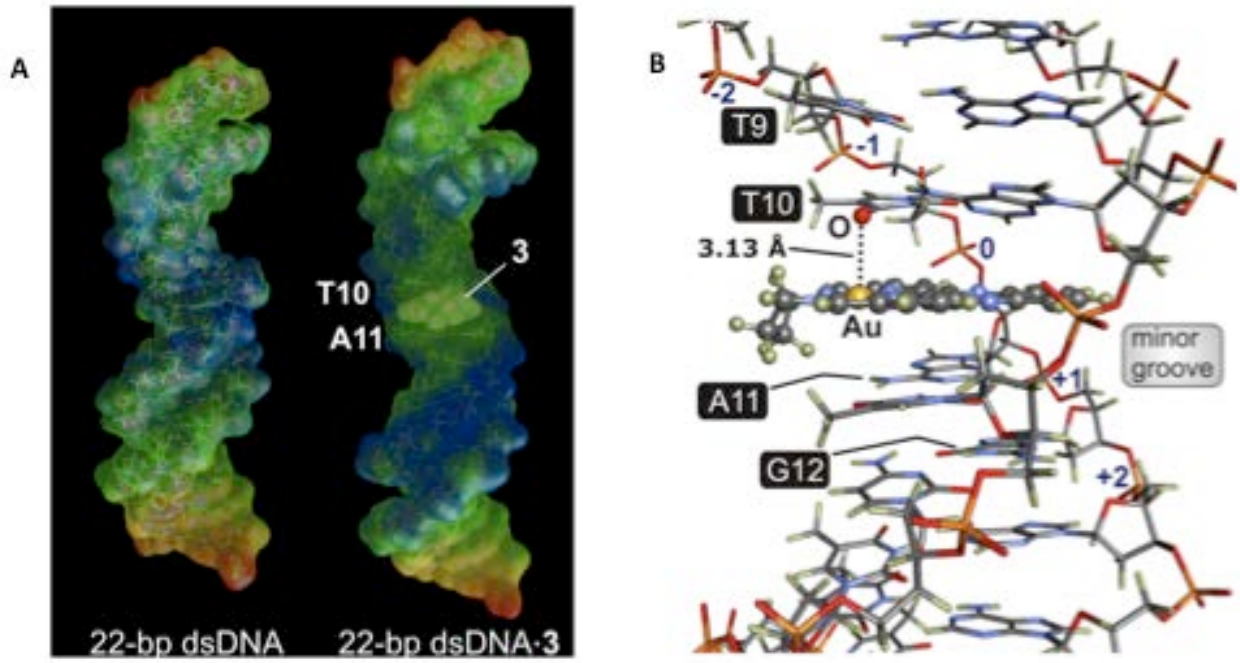

*This figure was produced by Dr. Munro in his molecular simulation studies

A) A molecular surface representation of the DNA in the absence and presence of the butyl gold(III) macrocycle (compound 3). The simulation reveals cmpd. 3 localized to a "TA" di-nucleotide site. When compound 3 is intercalated into the DNA, we observe local unwinding of the helix, as well as a change in the geometry of the DNA at the intercalation site. This simulation provides a molecular basis for why TOP1 and TOP2α cannot bind and cut DNA.

B) The specific interactions between compiund 3 and the DNA are shown with DNA represented in stick notation, and compound 3 in ball and stick notation. The critical interaction between the Au^{3+} and carbonyl of the T10 residue is shown, which allows for compound 3 to remain in a tight association with the DNA. The butyl gold(III) macrocycle also interacts with T10 and A11 through π-π stacking with the bases that further stabilizes the Drug-DNA complex.

An intercalation event at the enzyme cut-site, would classify the gold(III) macrocycle as a competitive inhibitor as the drug is competing with the enzyme for the same DNA sequence. It is possible that this is the case with some of the macrocycles, but an intercalation event at a di-nucelotide sequence distant from the cut-site could also inhibit the enzyme, which would be referred to as non-competitive inhibition. It is known that intercalation of the DNA produces local unwinding of the helix[22, 38, 39]. Given sufficient intercalation events it is possible to unwind the DNA enough to form a structure that sterically hinders enzyme access to the cleavage site. This is plausible and consistent with the DNA unwinding data (**Fig. 7**) demonstrates the gold (III) macrocycles unwind the DNA in a strong manner. Further simulation and crystallization experiments should confirm which intercalation mechanism is predominant.

Since the butyl gold(III) macrocycle (compound 3) forms a seven-membered ring in the linker region (denoted X in **Fig. 4**), the resulting confirmation causes the ring to bridge above and below the plane. All of the other macrocycles form a six-membered ring with no bridge; this slight difference in structure could be the reason as to why the butyl macrocycle is most cytotoxic in cells. The *in vitro* topoisomerase assays reveal compound 3 to act as a catalytic inhibitor in the same concentration range as compounds 1-5 (**Figs. 11 and 12**). This seven-membered ring formed in the butyl complex cannot be ignored, as it might have something to do with the enhanced cytotoxicity in the NCI-60 screen. The bridge created above and below the plane might fit the major groove of the DNA better

than the other macrocycles. Additionally it might also inhibit other essential DNA-binding enzymes that we are not aware of.

In the SPR experiments with the DNA bound chip in (**Fig. 9**), we observe a stronger binding affinity with the propyl gold(III) macrocycle (compound 1) than with the butyl gold(III) macrocycle (compound 3) yielding K_D values of 15.32 μM for compound 3 and 2.88 μM for compound 1. More interesting is the way the SPR response is seen qualitatively in (**Fig. 8**). With both compounds 1 and 3 a certain amount of drug binds, followed by a period of no detecable binding, then followed by further increase in the response curve (representing additional binding). This result is suggests multiple binding events on the target. The DNA helix unwinds upon a first intercalation, allowing additional molecules of drug to bind to distant sites. *In vivo* this could have a cooperativity effect where the binding of one drug influences additional binding downstream or upstream from the first intercalation site. The possibility of multiple binding and enhanced cooperativity is simply a speculation at this point, but working this out experimentally could lead to a valuable advancement in the knowledge of how these drugs work *in vivo.*

Described above are some possible reasons as to why the butyl gold(III) macrocycle (compound 3) is most cytotoxic in cells. Since the TOP1 assays do not reveal significant differences in IC_{50} values (**Fig. 11**), there must be a reason as to why there is a variable difference in cytotoxicity amongst the macrocycles within the NCI-60 screen. The mechanism by which the gold(III) macrocycles as a family of compounds that intercalate into DNA and inhibit TOP1 and TOP2α has been described. The main goals now lie in the

area of crystal structure and confirmation of the molecular mechanism *in vivo.* It is known that many cellular processes work differently *in vitro* than *in vivo*. Furthermore, there is a pressing need to study the macrocycles purely *in vivo* to see if there are other molecular targets.

The Au^{3+} ion does not readily dissociate out of the macrocyclic complex. Carrying an overall positive charge with a planar and hydrophobic backbone makes the drug a good candidate for traversing the cell membrane. However, this has not been studied experimentally and needs further evaluation. Certain drugs are known to enter the cell non-specifically via the transmembrane protein transporters[40-43]. This is the primary route of drug resistance, because cancer cells can mutate protein transporters that are unable to carry the drug. This is important because it is known that many drugs are active *in vitro*, but then the cell acts in such a way to metabolize the drug and render it inactive. This effect is seen with CPT, as the molecule can become inactivated in the "open-ring" lactone form. Further studies with cells should be carried out to assess the pharmacokinetics and dynamics of drug-uptake into cells.

Transitioning this compound into clinics will take time, but has a real potential to treat cancer. Most cancer drugs are genotoxic, resulting in massive DNA damage. Coupled to the genotoxic events is collateral damage to healthy cells such as cardiac cells, which is the case when patients are treated with doxorubucin, a TOP2α IFP[5]. A treatment strategy employed to reduce collateral treatment has been the synergism of doxorubucin with ICRF compounds[16]. The principle here is that some of the TOP2α molecules become locked in

the “closed-clamp” confirmation as the result of ICRF mediated catalytic inhibition. This prevents some TOP2α molecules from becoming lethal in the cell by forming DNA DSBs. This same strategy can be employed by treating patients with the gold macrocycle coupled with CPT, the TOP1 IFP.

Additionally, treating patients with the gold macrocycle independent of an IFP can result in cell killing with a less genotoxcicity as compared to other cancer chemotherapeutics. Treatment with the CIC can effectively inhibit TOP1 and TOP2α, which are both required for cell proliferation. By shutting off these essential enzymes, the cell will acquire a build up of topologically constrained DNA, and the accumulation of this DNA will signal for cell death.

In conclusion, a series of macrocyclic gold (III) complexes have been synthesized and studied extensively *in vitro*. The data reveal the complexes to have anti-tumor potential with a specific molecular mechanism. There is a desperate need for new anti-cancer agents in the clinic, and this class of compounds has serious potential. They should be studied extensively *in vivo* with animal models to evaluate the compounds in a setting similar to the human cancer patient. Moving to an animal model marks the next step to incorporating these compounds into the regiment of cancer chemotherapy.

Chapter 5: References

1. Pommier, Y., *Topoisomerase I inhibitors: camptothecins and beyond.* Nat Rev Cancer, 2006. **6**(10): p. 789-802.
2. Nitiss, J.L., *DNA topoisomerase II and its growing repertoire of biological functions.* Nat Rev Cancer, 2009. **9**(5): p. 327-37.
3. Strumberg, D., et al., *Molecular analysis of yeast and human type II topoisomerases. Enzyme-DNA and drug interactions.* J Biol Chem, 1999. **274**(40): p. 28246-55.
4. Morgan-Linnell, S.K., et al., *Assessing sensitivity to antibacterial topoisomerase II inhibitors.* Curr Protoc Pharmacol, 2007. **Chapter 3**: p. Unit3 13.
5. Pommier, Y., et al., *DNA topoisomerases and their poisoning by anticancer and antibacterial drugs.* Chem Biol, 2010. **17**(5): p. 421-33.
6. Kiselev, E., et al., *7-azaindenoisoquinolines as topoisomerase I inhibitors and potential anticancer agents.* J Med Chem, 2011. **54**(17): p. 6106-16.
7. Goto, T., P. Laipis, and J.C. Wang, *The purification and characterization of DNA topoisomerases I and II of the yeast Saccharomyces cerevisiae.* J Biol Chem, 1984. **259**(16): p. 10422-9.
8. Kirkegaard, K., G. Pflugfelder, and J.C. Wang, *The cleavage of DNA by type-I DNA topoisomerases.* Cold Spring Harb Symp Quant Biol, 1984. **49**: p. 411-9.
9. Berger, J.M., et al., *Structure and mechanism of DNA topoisomerase II.* Nature, 1996. **379**(6562): p. 225-32.
10. Nitiss, J.L., *Targeting DNA topoisomerase II in cancer chemotherapy.* Nat Rev Cancer, 2009. **9**(5): p. 338-50.
11. Aris, S.M. and Y. Pommier, *Potentiation of the Novel Topoisomerase I Inhibitor Indenoisoquinoline LMP-400 by the Cell Checkpoint and Chk1-Chk2 Inhibitor AZD7762.* Cancer Res, 2012. **72**(4): p. 979-89.
12. Andoh, T. and R. Ishida, *Catalytic inhibitors of DNA topoisomerase II.* Biochim Biophys Acta, 1998. **1400**(1-3): p. 155-71.
13. Pommier, Y., *DNA topoisomerase I inhibitors: chemistry, biology, and interfacial inhibition.* Chem Rev, 2009. **109**(7): p. 2894-902.
14. Wang, L. and D.A. Eastmond, *Catalytic inhibitors of topoisomerase II are DNA-damaging agents: induction of chromosomal damage by merbarone and ICRF-187.* Environ Mol Mutagen, 2002. **39**(4): p. 348-56.
15. Andoh, T., *Bis(2,6-dioxopiperazines), catalytic inhibitors of DNA topoisomerase II, as molecular probes, cardioprotectors and antitumor drugs.* Biochimie, 1998. **80**(3): p. 235-46.
16. Jensen, P.B. and M. Sehested, *DNA topoisomerase II rescue by catalytic inhibitors: a new strategy to improve the antitumor selectivity of etoposide.* Biochem Pharmacol, 1997. **54**(7): p. 755-9.

17. Pan, X., et al., *Evodiamine, a dual catalytic inhibitor of type I and II topoisomerases, exhibits enhanced inhibition against camptothecin resistant cells.* Phytomedicine, 2012.
18. Pommier, Y., et al., *The formation and resealing of intercalator-induced DNA strand breaks in isolated L1210 cell nuclei.* Biochem Biophys Res Commun, 1982. **107**(2): p. 576-83.
19. Capranico, G., et al., *Sequence-selective topoisomerase II inhibition by anthracycline derivatives in SV40 DNA: relationship with DNA binding affinity and cytotoxicity.* Biochemistry, 1990. **29**(2): p. 562-9.
20. Pommier, Y., et al., *DNA unwinding and inhibition of mouse leukemia L1210 DNA topoisomerase I by intercalators.* Nucleic Acids Res, 1987. **15**(16): p. 6713-31.
21. Poddevin, B., et al., *Dual topoisomerase I and II inhibition by intoplicine (RP-60475), a new antitumor agent in early clinical trials.* Mol Pharmacol, 1993. **44**(4): p. 767-74.
22. Pommier, Y., et al., *Effects of the DNA intercalators 4'-(9-acridinylamino)methanesulfon-m-anisidide and 2-methyl-9-hydroxyellipticinium on topoisomerase II mediated DNA strand cleavage and strand passage.* Biochemistry, 1985. **24**(23): p. 6410-6.
23. Leteurtre, F., et al., *Topoisomerase II inhibition and cytotoxicity of the anthrapyrazoles DuP 937 and DuP 941 (Losoxantrone) in the National Cancer Institute preclinical antitumor drug discovery screen.* J Natl Cancer Inst, 1994. **86**(16): p. 1239-44.
24. Guano, F., et al., *Topoisomerase poisoning activity of novel disaccharide anthracyclines.* Mol Pharmacol, 1999. **56**(1): p. 77-84.
25. Godwin, A.K., et al., *High resistance to cisplatin in human ovarian cancer cell lines is associated with marked increase of glutathione synthesis.* Proc Natl Acad Sci U S A, 1992. **89**(7): p. 3070-4.
26. Siddik, Z.H., *Cisplatin: mode of cytotoxic action and molecular basis of resistance.* Oncogene, 2003. **22**(47): p. 7265-79.
27. Ronconi, L., et al., *Gold(III) dithiocarbamate derivatives for the treatment of cancer: solution chemistry, DNA binding, and hemolytic properties.* J Med Chem, 2006. **49**(5): p. 1648-57.
28. Palanichamy, K., M. Erkkinen, and A. Chakravarti, *Predictive and prognostic markers in human glioblastomas.* Curr Treat Options Oncol, 2006. **7**(6): p. 490-504.
29. Yan, J.J., et al., *Cyclometalated gold(III) complexes with N-heterocyclic carbene ligands as topoisomerase I poisons.* Chem Commun (Camb), 2010. **46**(22): p. 3893-5.
30. Che, C.M., et al., *Gold(III) porphyrins as a new class of anticancer drugs: cytotoxicity, DNA binding and induction of apoptosis in human cervix epitheloid cancer cells.* Chem Commun (Camb), 2003(14): p. 1718-9.
31. Palanichamy, K., N. Sreejayan, and A.C. Ontko, *Overcoming cisplatin resistance using gold(III) mimics: anticancer activity of novel gold(III) polypyridyl complexes.* J Inorg Biochem, 2012. **106**(1): p. 32-42.
32. Stewart, L. and J.J. Champoux, *Purification of baculovirus-expressed human DNA topoisomerase I.* Methods Mol Biol, 1999. **94**: p. 223-34.

33. Lindsley, J.E., *Overexpression and purification of Saccharomyces cerevisiae DNA topoisomerase II from yeast.* Methods Mol Biol, 1999. **94**: p. 187-97.
34. Andersen, A.H., et al., *Topoisomerase-I Has a Strong Binding Preference for a Conserved Hexadecameric Sequence in the Promotor Region of the Ribosomal-Rna Gene from Tetrahymena-Pyriformis.* Nucleic Acids Res, 1985. **13**(5): p. 1543-1557.
35. Waring, M.J., *DNA Modification and Cancer.* Annu Rev Biochem, 1981. **50**: p. 159-192.
36. Leteurtre, F., et al., *Specific interaction of camptothecin, a topoisomerase I inhibitor, with guanine residues of DNA detected by photoactivation at 365 nm.* Biochemistry, 1993. **32**(34): p. 8955-62.
37. Tlili, A., et al., *Electrical characterization of a thiol SAM on gold as a first step for the fabrication of immunosensors based on a quartz crystal microbalance.* Sensors, 2004. **4**(6-7): p. 105-114.
38. Capranico, G. and M. Binaschi, *DNA sequence selectivity of topoisomerases and topoisomerase poisons.* Biochim Biophys Acta, 1998. **1400**(1-3): p. 185-94.
39. Pommier, Y., et al., *Role of DNA intercalation in the inhibition of purified mouse leukemia (L1210) DNA topoisomerase II by 9-aminoacridines.* Biochem Pharmacol, 1987. **36**(20): p. 3477-86.
40. Pommier, Y. and M. Cushman, *The indenoisoquinoline noncamptothecin topoisomerase I inhibitors: update and perspectives.* Mol Cancer Ther, 2009. **8**(5): p. 1008-14.
41. Sooryakumar, D., et al., *Molecular and cellular pharmacology of the novel noncamptothecin topoisomerase I inhibitor Genz-644282.* Mol Cancer Ther, 2011. **10**(8): p. 1490-9.
42. Zhang, Y.W., et al., *Implication of checkpoint kinase-dependent up-regulation of ribonucleotide reductase R2 in DNA damage response.* J Biol Chem, 2009. **284**(27): p. 18085-95.
43. Pommier, Y., et al., *Cellular resistance to camptothecins.* Ann N Y Acad Sci, 1996. **803**: p. 60-73.